

Mott insulators with large local Hilbert spaces in quantum materials and ultracold atoms

Gang Chen*

Department of Physics and HKU-UCAS Joint Institute for Theoretical and Computational Physics at Hong Kong, The University of Hong Kong, Hong Kong, China

Congjun Wu†

*School of Science, Westlake University, Hangzhou 310024, Zhejiang, China
Institute for Theoretical Sciences, Westlake University, Hangzhou 310024, Zhejiang, China and
Key Laboratory for Quantum Materials of Zhejiang Province,
School of Science, Westlake University, Hangzhou 310024, China*

(Dated: December 7, 2021)

Mott insulators with large local Hilbert spaces (or multicomponent local Hilbert spaces) appear widely in quantum materials and ultracold atomic systems. For the Mott insulating quantum materials with a large local Hilbert space, the spin-only description with pairwise quadratic spin interactions is often insufficient to capture the interaction. In the situation with active local orbital degrees of freedom, the Kugel-Khomskii superexchange model was then proposed. We here briefly review this historical model and discuss the modern arenas and developments beyond the original orbital context where this model and the relevant physics emerge. These include and are not restricted to the $4d/5d$ transition metal compounds with the spin-orbital-entangled $J = 3/2$ quadruplets, the rare-earth magnets with two weakly separated crystal field doublets, breathing magnets and/or the cluster and molecular magnets, *et al.* We explain the microscopic origin of the emergent Kugel-Khomskii physics in each solid-state realization with some emphasis on the $J = 3/2$ quadruplets, and dub the candidate systems “ $J = 3/2$ Mott insulators”. For the ultracold atom contexts, we review the Mott insulators with the large-spin ultracold alkaline and alkaline-earth atoms on the optical lattices, where a large local Hilbert space naturally emerges. Despite a large local Hilbert space from the atomic hyperfine spin states, the system could realize a large symmetry group such as the $Sp(N)$ or the $SU(N)$ symmetry. These ultracold atomic systems actually lie in the large- N regime of large symmetry groups and are characterized by strong quantum fluctuations. The Kugel-Khomskii physics and the exotic quantum ground states with the “bayone-like” physics can appear in various limits. We conclude with our vision and outlook on this subject.

I. INTRODUCTION

There are many ways to classify and view the physics related to correlated many-body systems [1]. One classification scheme may be considered insufficient and thus misses other complementary views, and different views could raise different types of questions and point to new directions of our field. Here we sketch some popular schemes and views in the field. One could classify the quantum many-body systems from the relevant and emergent phases and phase transitions. Alternatively, one could summarize various physical phenomena and classify the qualitative behaviors that may or may not be unique to particular phases. One can further identify the internal structures of the underlying systems such as intrinsic topological structures [2] or emergent symmetries and the related experimental signatures. One may also discuss various universal properties pertinent to certain phases or focus on the physical realization of these phases in quantum materials with the relevant physical degrees of freedom. The last view may necessarily involve a significant amount of specific physics and specific features of the degrees of freedom and the underlying quantum materials [3, 4]. The universal parts of the physics, however, are inevitably entangled with the specific physics and manifest themselves in terms of the specific degrees of

freedom. The balance between universality and specifics may be strongly constrained by the specific materials instead of being determined by the subjective purposes. Therefore, one could further classify the correlated many-body systems according to the relevant physical degrees of freedom and their interactions.

With the above thoughts, we turn our attention to the Mott insulators with large local Hilbert spaces. Such systems were also referred as Mott systems with multicomponent local Hilbert spaces [5]. We will use the former terminology in this review. One traditional example of such Mott systems is the one involving both active spin and orbital degrees of freedom for which the Kugel-Khomskii spin-orbital superexchange model was proposed by Kliment Kugel and Daniel Khomskii [6]. The advance they made beyond the Anderson’s mechanism [7] of the superexchange spin interaction was to include the orbital degrees of freedom and treat them on an equal footing as the spin degrees of freedom. The resulting model was later referred as the Kugel-Khomskii model and involves the spin exchange, the orbital exchange and the spin-orbital exchange interactions. Because of the complicated expression and the orbital involvement, the Kugel-Khomskii model did not receive a significant attention over the past few decades. Nevertheless, the Kugel-Khomskii physics is real and relevant for many physical systems [3, 4, 8–10]. In the recent years, the orbital degrees of freedom and the orbital related physics are receiving more attention. This is due to many factors, such as the emergence of topological materials [11–14] (that often require the spin-orbit coupling to generate the

* gangchen@hku.hk

† wucongjun@westlake.edu.cn

topological band structures), the spin-orbit-coupled correlated materials where the spin-orbit coupling is the key ingredient [15], the experimental progress including the resonant X-ray scattering measurement that allows the experimental detection of the orbital physics [16, 17], and so on. Therefore, it is timing to explore the Kugel-Khomskii physics and bring it back to the attention of the community. Part of this review aims to suggest the broad applicability of the Kugel-Khomskii model in the Mott insulating quantum materials with a large local Hilbert space beyond the original spin-orbital disentangled context. By “disentangled”, we mean that the spins and the orbitals are locally independent variables. The new territory for the Kugel-Khomskii physics is proposed to be the emerging Mott insulating systems with a large local Hilbert space. This includes, but is not restricted to, the breathing materials and/or cluster and molecular magnets, the rare-earth magnets with weak crystal fields, the spin-orbital-entangled $J = 3/2$ local moments of transition metal compounds, *etc.* Beyond the condensed matter contexts, the ultracold atom systems, such as the alkaline atoms and the alkaline-earth atoms on the optical lattices, could serve as candidate systems to realize the Kugel-Khomskii physics together with their own merits with the high symmetry groups that are discussed in the second half of the review.

The observation is that, despite the proposed contexts do not explicitly contain the orbital degrees of freedom like the original Kugel-Khomskii context, there exist emergent orbital-like degrees of freedom that play the role of the orbitals. For the breathing magnets and/or cluster Mott systems [18–28], it is the degenerate ground states of the local clusters that function as effective orbitals. The effective Kugel-Khomskii physics appears when one considers the residual interactions between the degenerate ground states of the local clusters. These interactions lift the remaining degeneracy and create the many-body ground states. For certain rare-earth magnets [29–34], although the orbitals are present implicitly, they are strongly entangled with the spin degrees of freedom, and then what is meaningful is the local “ J ” moment. For this case, it is the degenerate energy levels that can be treated as effective orbital degrees of freedom. For the transition metal compounds with the $J = 3/2$ local moments that are dubbed “ $J = 3/2$ Mott insulators” [25, 35–40], one can group the four local states into two fictitious orbitals with one spin-1/2 moment and then naturally describe the interaction as the Kugel-Khomskii model. We carefully derive the superexchange model in terms of the effective spin and orbital degrees of freedom and express the model in the form of the Kugel-Khomskii interaction. The derivation is delivered through a honeycomb lattice structure. The correspondence between the microscopic multipolar moments in the $J = 3/2$ language and the effective spin-orbital language is established. This correspondence may be useful for the mutual feedback between the understanding from different languages and views. This $J = 3/2$ local moments and the effective Kugel-Khomskii physics can be broadly applied to many $4d/5d$ Mott systems such as the Mo-base, Re-based, Os-based double perovskites [35], and can even be relevant to certain $3d$ transition metal compounds such as vanadates with the V^{4+}

ions [3, 41].

We devote the second half of the review to the ultracold atom system. The ultracold atom system has become a new frontier of condensed matter physics and provides new opportunities and platforms for exploring the novel correlation physics. The Kugel-Khomskii physics turns out to be particularly relevant for many alkali and alkaline-earth atoms [42]. These atoms possess large hyperfine spins, and their physical picture is very much different from that of traditional magnets with large spins. Here, the traditional magnets refer to the conventional $3d$ transition metal compounds without quenched orbitals [3] and are used to distinguish from the ones discussed in the previous paragraphs. In these traditional magnets, large spins arise from the Hund’s coupling: the spins of the localized electrons on the same transition metal ions are aligned to form a large spin. The leading order contribution to the couplings between different sites is the superexchange of a single pair of electrons, such that the fluctuation with respect of an ordered moment would be just ± 1 . This is the physical origin of the $1/S$ -effect, in other words, as S is enlarged, the system evolves towards the classical direction. However, in many alkali and alkaline-earth atom systems, the situation is quite different. This is a bit analogous to the situation in the “ $J = 3/2$ Mott insulator”. The energy scale is far below the atomic ionization energy, and exchanging a pair of fermions can completely shuffle the spin configuration among the $2S + 1$ spin states. The spin states are much more delocalized in their Hilbert space. Thus, a large spin here behaves more like a large number of components, which strongly enhances the quantum fluctuations. It is more appropriate to adopt the perspective of high symmetries (e.g., $SU(N)$ and $Sp(N)$ with $N = 2S + 1$) [43–49].

This new perspective from these ultracold atom systems provides an opportunity to explore the many-body physics closely related to the Kugel-Khomskii-like physics for $N = 4$, and some aspects with high symmetries may even be connected to the high-energy physics. As an early progress, an exact and generic symmetry of $Sp(4)$, or, isomorphically $SO(5)$, was proved in the spin-3/2 alkali fermion systems [43, 44]. Under the fine-tuning, the $Sp(4)$ symmetry can be augmented to $SU(4)$. Later, the $SU(N)$ symmetry has also been widely investigated in the alkaline-earth fermion systems [42, 50, 51]. For instance, the alkaline-earth-like atom ^{173}Yb with spin $S = 5/2$ [49] has 6 components, and the ^{87}Sr atom with $S = 9/2$ [48] has 10 spin components, respectively.

We will review the novel properties of quantum magnetism with ultracold atoms possessing the $Sp(N)$ and $SU(N)$ symmetries with $N = 4$. These are the ultracold-atom versions of the Kugel-Khomskii physics. They are characterized by various competing orders due to the strong quantum fluctuations. As an exotic example, they can exhibit the “baryon-like” physics. In an $SU(4)$ quantum magnet, quantum spin fluctuations are dominated by the multi-site correlations, whose physics is beyond the two-site one of the $SU(2)$ magnets as often studied in the condensed matter systems. It is exciting that in spite of the huge difference of the energy scales, the large-spin cold fermions can also exhibit similar physics to quantum chromodynamics (QCD).

The remaining parts of this review are organized as follows. In Sec. II, we start with a brief introduction of the original proposal of the Kugel-Khomskii superexchange model in the large-local-Hilbert-space Mott insulating systems with active orbitals. In Sec. III, we explain various solid-state realizations of the Kugel-Khomskii physics and the status of the effective orbitals. In Sec. IV, we turn the attention to the “ $J = 3/2$ ” Mott insulators and establish the Kugel-Khomskii physics. In Sec. V, we review the ultracold atoms on optical lattices and discuss the high-symmetry models and the emergent physics with the alkaline and alkaline earth atoms. Finally, in Sec. VI, we summarize this reviews.

II. KUGEL-KHOMSKII EXCHANGE MODEL IN MOTT INSULATORS

As we have remarked in Sec. I, a conventional and representative example of the Mott insulators with a large local Hilbert space is the one involving active orbital degrees of freedom. We start the review with these spin-orbital-based Mott insulators and their superexchange interactions.

The Anderson superexchange interaction for the spin degrees of freedom in the Mott insulators is widely accepted as the major mechanism for the antiferromagnetism [7]. Anderson’s treatment was perturbative. The virtual exchange of the localized electrons from the neighboring sites through the high-order perturbation processes generates a Heisenberg interaction between the local spin moments. Anderson’s original work was based on a single-band Hubbard model where only one orbital related band is involved, and Anderson’s treatment could be well adjusted to include the orbitals from the intermediate anions. Insights from these calculations were summarized as the empirical Goodenough-Kanamori-Anderson (GKA) rules [52, 53].

For the Hubbard model with multiple orbitals at the magnetic ions, the orbital necessarily becomes an active degree of freedom in addition to the spin once the system is in the Mott insulating phase with localized electrons on the lattice sites [6]. In this case, more structures are involved in the local moment formation that generates a large local Hilbert space with both spins and orbitals in the Mott regime, and the original Anderson’s spin exchange cannot be directly applied here. With more active degrees of freedom in the large local physical Hilbert space, the GKA rules can no longer provide the nature and the magnitude of the exchange interactions, even the signs of the exchange interactions cannot be determined. These exchange interactions sensitively depend on the orbital configurations on each lattice site. Moreover, as the orbital is an active and dynamical degree of freedom here, the orbitals are intimately involved in the superexchange processes. Thus, in addition to the exchange of the spin quantum numbers, the perturbative superexchange processes in these Mott insulators are able to exchange the orbital quantum numbers. In reality, both the spin and the orbital quantum numbers can be exchanged separately or simultaneously. Taking together, the full exchange Hamiltonian would involve pure spin exchange, pure orbital exchange, and the mixed spin-orbital ex-

change [6]. This spin-orbital exchange model is nowadays referred as “Kugel-Khomskii model”.

Closely following Kugel and Khomskii [6], we present an illustrative derivation of the Kugel-Khomskii spin-orbital exchange model from a two-orbital Hubbard model. The Hubbard model is given [6],

$$H = \sum_{\langle ij \rangle} t_{ij}^{\alpha\beta} a_{i\alpha\sigma}^\dagger a_{j\beta\sigma} + \frac{1}{2} \sum_i U_{\alpha\beta} n_{i\alpha\sigma} n_{i\beta\sigma'} (1 - \delta_{\alpha\beta} \delta_{\sigma\sigma'}) - \frac{1}{2} \sum_{i,\alpha\neq\beta} J_H (a_{i\alpha\sigma}^\dagger a_{i\alpha\sigma'} a_{i\beta\sigma'}^\dagger a_{i\beta\sigma} + a_{i\alpha\sigma}^\dagger a_{i\beta\sigma} a_{i\alpha\sigma'}^\dagger a_{i\beta\sigma'}), \quad (1)$$

where $\alpha, \beta = 1, 2$ label the two orbitals, σ, σ' label the spin quantum number, and the final term takes care of the inter-orbital pair hopping and the Hund’s coupling. The orbital degeneracy is assumed, and an isotropic and diagonal hopping $t_{11} = t_{22} = t, t_{12} = 0$ is further assumed. In reality, the isotropic and diagonal hoppings are not guaranteed, and the orbital degeneracy is not quite necessary. A standard perturbation treatment yields the conventional Kugel-Khomskii model with

$$H_{KK} = \sum_{\langle ij \rangle} J_1 \mathbf{S}_i \cdot \mathbf{S}_j + J_2 \boldsymbol{\tau}_i \cdot \boldsymbol{\tau}_j + 4J_3 (\mathbf{S}_i \cdot \mathbf{S}_j) (\boldsymbol{\tau}_i \cdot \boldsymbol{\tau}_j), \quad (2)$$

where we have the relations,

$$\sum_{\sigma} a_{i,1,\sigma}^\dagger a_{i,1,\sigma} = \frac{1}{2} + \tau_i^z, \quad (3)$$

$$\sum_{\sigma} a_{i,2,\sigma}^\dagger a_{i,2,\sigma} = \frac{1}{2} - \tau_i^z, \quad (4)$$

$$\sum_{\sigma} a_{i,1,\sigma}^\dagger a_{i,2,\sigma} = \tau_i^+, \quad (5)$$

$$\sum_{\sigma} a_{i,2,\sigma}^\dagger a_{i,1,\sigma} = \tau_i^-, \quad (6)$$

and

$$\sum_{\alpha} a_{i,\alpha,\uparrow}^\dagger a_{i,\alpha,\uparrow} = \frac{1}{2} + S_i^z, \quad (7)$$

$$\sum_{\alpha} a_{i,\alpha,\downarrow}^\dagger a_{i,\alpha,\downarrow} = \frac{1}{2} - S_i^z, \quad (8)$$

$$\sum_{\alpha} a_{i,\alpha,\uparrow}^\dagger a_{i,\alpha,\downarrow} = S_i^+, \quad (9)$$

$$\sum_{\alpha} a_{i,\alpha,\downarrow}^\dagger a_{i,\alpha,\uparrow} = S_i^-, \quad (10)$$

and the exchange couplings are given as

$$J_1 = \frac{2t^2}{U} (1 - \frac{J_H}{U}), \quad (11)$$

$$J_2 = J_3 = \frac{2t^2}{U} (1 + \frac{J_H}{U}). \quad (12)$$

Because the spin and orbitals are disentangled, the spin sector retains the SU(2) rotational symmetry. The orbital SU(2) symmetry in Eq. (2) is accidental and is due to the special choice of the hopping parameters. Via a fine-tuning of the hoppings

and the interactions, the Kugel-Khomskii model could have a larger symmetry such as $SU(4)$ [54], and the limit with a higher symmetry may provide a new solvability of this complicated but realistic model.

In the above derivation of the Kugel-Khomskii model, the orbital degeneracy is not actually required. As long as the crystal field splitting between the orbitals is small or comparable to exchange energy scale, we need to seriously include the orbitals into the description of the correlation physics for the local moments in the Mott regime. This would clear up the unnecessary constraint of the Kugel-Khomskii physics to the Mott systems with an explicit orbital degeneracy. A perfect orbital degeneracy requires a high crystal field symmetry and is not quite common. The clearance of this constraint would expand the applicability of the Kugel-Khomskii physics in the transitional metal compounds.

From the above example, one could readily extract some of the essential properties for the Kugel-Khomskii model and the related physics for the Mott insulators with active spins and orbitals. As the orbitals have the spatial orientations in the real space, the electron hopping between the orbitals from the neighboring sites depends strongly on the bond orientation and the orbital configurations. The resulting Kugel-Khomskii model is anisotropic in the orbital sector, and the exchange interaction depends on the bond orientations. Because the spin and the orbital are disentangled in the parent Hubbard model and the spin-orbit coupling is not considered, the spin interaction in the spin sector, however, remains isotropic in the Kugel-Khomskii model and is described by the conventional Heisenberg interaction. For the relevant transition metal compounds, the common orbital degrees of freedom can be e_g and t_{2g} orbitals. In the case of the e_g orbitals, an effective pseudospin-1/2 operator is often used to label the orbital state [6], and this corresponds to the situation in the above example. For the t_{2g} orbitals, a pseudospin-1 operator is used to label the three t_{2g} orbitals [55, 56], and the corresponding Kugel-Khomskii model is much more involved. The local physical Hilbert space is significantly enlarged by the orbital degrees of freedom. The Kugel-Khomskii model operates quite effectively in this enlarged local Hilbert space. This is quite different from the spin-only Mott insulators with a large- S local spin moment where the orbital degree of freedom is quenched. Although the physical Hilbert space is enlarged with a large- S local spin moment, the simple Heisenberg spin model merely changes the spin quantum number by 1 with one operation. In contrast, the Kugel-Khomskii spin-orbital model is more effectively in delocalizing the spin-orbital states in the enlarged physical Hilbert space and thus enhances the quantum fluctuations.

III. MODERN SOLID-STATE REALIZATION OF EMERGENT KUGEL-KHOMSKII PHYSICS

In the previous section, we have demonstrated that the original Kugel-Khomskii model can be derived from an extended Hubbard model with multiple orbitals. Orbital degeneracy is often assumed but not necessarily required. If the orbital sepa-

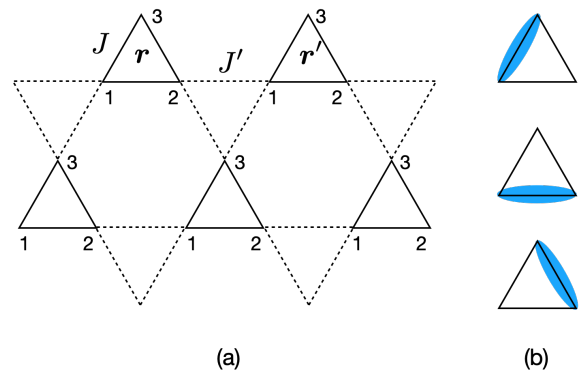


FIG. 1. (a) The breathing kagomé lattice structure with an alternating exchange coupling on the triangular cluster. (b) The three configurations of the spin singlet occupation on the triangular cluster. The (blue) dimer refers to the spin singlet of two spins, and the uncovered site is the dangling spin moment. Two of the three configurations are linearly independent. There are totally four ground states of the triangular cluster after including the two fold degeneracy of the dangling spin.

ration is of the energy scale as the superexchange energy scale, then one should carefully include these orbitals into our modeling. Depending on the electron filling, the spin moment can be spin-1/2 and spin-1, and the pseudospin for the orbital sector can be pseudospin-1/2 (for e_g degeneracy, or two-fold t_{2g} degeneracy) and pseudospin-1 (for three-fold t_{2g} degeneracy). The spin and orbitals are disentangled in this model.

A well-known example would be the Fe-based superconductors [57–59]. Although the parent materials behave mostly like a bad metal and are thus modeled by an extended Hubbard model with multiple electron orbitals, many important physics such as the magnetic excitations and spectra may be better understood from the local moment picture. This was used to interpret the magnetic excitations in FeSe that is believed to be the most “Mott”-like Fe-based superconducting system [60, 61]. The active orbital degree of freedom in FeSe, however, has not been included into the analysis of the magnetic properties and the excitations [62]. Thus, FeSe can be a good application of the original Kugel-Khomskii model for the understanding of the magnetism, the orbital physics and the nematicity [63–65].

While the Kugel-Khomskii model is proposed for the spin-orbital disentangled Mott insulators, we explain its broad application to other systems below.

A. Breathing magnets and cluster magnets

Breathing magnets (and cluster magnets) represent a new family of magnetic materials whose building blocks are not the magnetic ions, and can find their applications in many organic magnets [66, 67] and even inorganic compounds [68]. Instead, the systems consist of the magnetic cluster units as the building blocks, and these magnetic cluster units provide the elementary and local degrees of freedom for the magnetism. To understand the physics of these systems, one ought

to first understand the local physics on the cluster unit and find the relevant low-energy states. The many-body model for the system should be constructed from these relevant local low-energy states. To illustrate the point above, we notice that the early spin liquid candidate κ -(ET)₂Cu₂(CN)₃ can actually be placed into the category of the cluster magnets [69]. In κ -(ET)₂Cu₂(CN)₃, each (ET)₂ molecular dimer hosts odd number of electrons. As the molecular dimers form a triangular lattice, it was proposed that this model realizes the triangular lattice Hubbard model at the half filling. The basis of the Hamiltonian is the Wannier functions associated with the antibonding states of the highest occupied molecular orbitals on each (ET)₂ dimer [70]. More generally, the local energy levels of the magnetic clusters should be understood or classified from the irreducible representation of the local symmetry group, and the effective orbital degrees of the freedom on the cluster is then interpreted as the local basis of the irreducible representation [18, 19, 25].

To deliver the idea of the effective orbital degree of freedom, we start from the breathing kagomé lattice (see Fig. 1), and assume the simple Heisenberg interactions with alternating couplings,

$$H = J \sum_{\langle ij \rangle \in \Delta} \mathbf{S}_i \cdot \mathbf{S}_j + J' \sum_{\langle ij \rangle \in \nabla} \mathbf{S}_i \cdot \mathbf{S}_j, \quad (13)$$

where “ Δ ” (“ ∇ ”) refers to the up (down) triangles. The word “breathing” refers to the fact that the “ Δ ” triangles are of different size from the “ ∇ ” triangles and was first used in the context of the breathing pyrochlore magnets [71]. In the strong breathing limit with $J \gg J'$, one should first consider the local states on the up triangles and couple these local states together through the J' -links on the down triangles. On each up triangles, there are three spin-1/2 local moments. With the antiferromagnetic interactions, the ground states have four fold degeneracies. This can be understood simply from the spin multiplication relation with

$$\frac{1}{2} \otimes \frac{1}{2} \otimes \frac{1}{2} = \frac{1}{2} \oplus \frac{1}{2} \oplus \frac{3}{2}, \quad (14)$$

where the left hand side refers to the three spin local moments on the up triangle and the right hand side refers to the spin quantum number of the total spin of the up triangular cluster. The total spin, $S_{\text{tot}} = 3/2$, is only favored if the interaction is ferromagnetic. The antiferromagnetic spin interaction favors a total spin $S_{\text{tot}} = 1/2$, that is realized by forming a spin singlet between two spins and leaving the remaining spin as a dangling spin (see Fig. 1). This would naively lead to three singlet occupation configurations. It turns out that only two of them are linearly independent. Counting the spin-up and spin-down degeneracy of the dangling spin, there are in total four fold ground state degeneracies on each up triangular cluster. To make connection with the Kugel-Khomskii physics, one can simply regard the total spin of the up-triangle cluster as the effective spin, and regard the two-fold degeneracy of the spin singlet configuration as the effective orbital. The later has

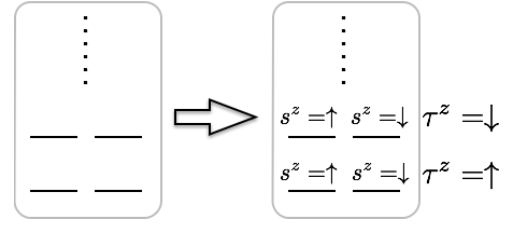


FIG. 2. The assignment of the effective spin and orbital to the local crystal field states of rare-earth moments. This applies to the Tb³⁺ ion in Tb₂Ti₂O₇, Tb₂Sn₂O₇ and others.

the spirit of an orbital as both are even under time reversal.

$$\begin{aligned} |s^z = \uparrow, \tau^z = \uparrow\rangle &= \frac{1}{\sqrt{3}} [|\downarrow_1 \uparrow_2 \uparrow_3\rangle + e^{i\frac{2\pi}{3}} |\uparrow_1 \downarrow_2 \uparrow_3\rangle + e^{-i\frac{2\pi}{3}} |\uparrow_1 \uparrow_2 \downarrow_3\rangle], \\ |s^z = \uparrow, \tau^z = \downarrow\rangle &= \frac{1}{\sqrt{3}} [|\downarrow_1 \uparrow_2 \uparrow_3\rangle + e^{-i\frac{2\pi}{3}} |\uparrow_1 \downarrow_2 \uparrow_3\rangle + e^{i\frac{2\pi}{3}} |\uparrow_1 \uparrow_2 \downarrow_3\rangle], \\ |s^z = \downarrow, \tau^z = \uparrow\rangle &= \frac{1}{\sqrt{3}} [|\uparrow_1 \downarrow_2 \downarrow_3\rangle + e^{-i\frac{2\pi}{3}} |\downarrow_1 \uparrow_2 \downarrow_3\rangle + e^{i\frac{2\pi}{3}} |\downarrow_1 \downarrow_2 \uparrow_3\rangle], \\ |s^z = \downarrow, \tau^z = \downarrow\rangle &= \frac{1}{\sqrt{3}} [|\downarrow_1 \uparrow_2 \uparrow_3\rangle + e^{-i\frac{2\pi}{3}} |\uparrow_1 \downarrow_2 \uparrow_3\rangle + e^{i\frac{2\pi}{3}} |\uparrow_1 \uparrow_2 \downarrow_3\rangle]. \end{aligned}$$

One then includes the J' interaction between the up-triangular clusters, and the resulting model is a Kugel-Khomskii model that is of the following form [72],

$$\begin{aligned} H_{\text{KK}} = \frac{4J'}{9} \sum_{\langle rr' \rangle} (\mathbf{s}_r \cdot \mathbf{s}_{r'}) & \left[\frac{1}{2} - (\alpha_{rr'} \tau_r^- + \alpha_{rr'}^* \tau_r^+) \right] \\ & \times \left[\frac{1}{2} - (\beta_{rr'} \tau_r^- + \beta_{rr'}^* \tau_r^+) \right], \quad (15) \end{aligned}$$

where \mathbf{r} refers to the center of the up-triangular cluster, and \mathbf{s}_r defines the total spin on the up-triangular cluster at \mathbf{r} . The parameters $\alpha_{rr'}$ and $\beta_{rr'}$ are the bond-dependent phase factors that are consistent with the orbital-like nature of the pseudospin τ . It is found that [72], the factor $\alpha_{rr'}$ equals to 1, $e^{i4\pi/3}$, or $e^{i2\pi/3}$ when the J' -coupled bond connects two neighboring up-triangles at \mathbf{r} and \mathbf{r}' from the spin 1, 2, 3 on the \mathbf{r} triangle, respectively. Similarly, the factor $\beta_{rr'}$ equals to 1, $e^{i4\pi/3}$, or $e^{i2\pi/3}$ when the J' -coupled bond connects two neighboring up-triangles at \mathbf{r} and \mathbf{r}' to the spin 1, 2, 3 on the \mathbf{r}' triangle, respectively.

Apart from the breathing kagomé magnet here, the breathing pyrochlore magnet can also be understood in a similar fashion. A recent interest of the breathing pyrochlore magnet is Ba₃Yb₂Zn₅O₁₁ that is in the strong breathing limit. Due to the strong spin-orbit coupling of the Yb 4f electrons, the local Hamiltonian on the smaller tetrahedron is not a simple Heisenberg model. Nevertheless, the understanding from the irreducible representation of the tetrahedral group should still be applicable and has already been applied to the experiments [28].

B. Rare-earth magnets with weak crystal field

It is a bit hard to imagine that the rare-earth magnets are described by the Kugel-Khomskii model. Usually, the rare-earth local moments are described by some effective spin-1/2 degrees of freedom, and this two-fold degeneracy is protected by time reversal symmetry and Kramers theorem for the non-Kramers doublet, and by the point group symmetry for the Kramers doublet, and by the point group symmetry for the non-Kramers doublet. For the rare-earth local moments, the orbital degrees of freedom have already been considered from the atomic spin-orbit coupling that entangles the atomic spin with the orbitals and leads to total moment “ J ”. The effective spin-1/2 doublet arises from the crystal field ground state levels of the total moment J . The low-energy magnetic physics is often understood from the interaction between the effective spin-1/2 local moments. This paradigm works rather well for the pyrochlore rare-earth magnets and the triangular lattice rare-earth magnets. The reason for the success of the paradigm is due to the large crystal field gap between the ground state doublet and the excited ones in the relevant materials. If this precondition breaks down, then we need to think about other resolution.

For the Tb^{3+} ion in $Tb_2Ti_2O_7$ and $Tb_2Sn_2O_7$ [29–33, 73–75], it is known that the crystal field energy gap between the ground state doublet and the first excited doublet is not very large compared to the Curie-Weiss temperatures in these systems. Thus the ground state doublet description is insufficient to capture the low temperature magnetic properties. This regime is quoted as “weak crystal field magnetism” in Ref. 34. Both the ground state doublet and the first excited doublet should be included into the microscopic model. To think along the line of the Kugel-Khomskii physics, we assign the energy levels with effective spin and effective orbital configurations. Here the two effective orbitals are separated by a crystal field energy gap. The exchange interaction between the local moments would be of Kugel-Khomskii-like. We expect other rare-earth magnets beyond $Tb_2Ti_2O_7$ and $Tb_2Sn_2O_7$ could share a similar physics from the perspective of Kugel-Khomskii.

C. $J = 3/2$ Mott insulator

What is “ $J = 3/2$ Mott insulator”? To present this notion, we begin with the notion of “ $J = 1/2$ Mott insulator” that seems to be quite popular in recent years [56, 76, 77]. The $J = 1/2$ Mott insulator was proposed to be relevant to various iridates, α - $RuCl_3$ [78], and even the Co-based $3d$ transition metal compounds [79–83]. This can be understood from the Ir^{4+} ion under the octahedral crystal field environment [56, 77]. The t_{2g} and e_g levels for single electron states are split by a large crystal field gap. When the spin-orbit coupling (SOC) is switched on, the t_{2g} orbital is entangled with the spin degree of freedom, leading to an upper $J = 1/2$ doublet and a lower $J = 3/2$ quadruplet. The Ir^{4+} ion has a $5d^5$ electronic configuration such that the lower quadruplet is fully filled and the upper doublet is half-filled. In the Mott insulating phase, the local moment is simply described by the

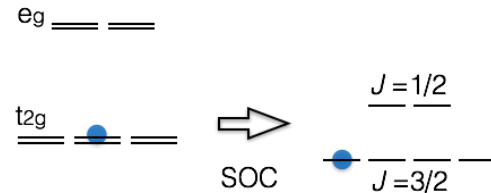


FIG. 3. The splitting of the *single* electron state under the spin-orbit coupling. The left is the crystal field scheme in the octahedral environment. The right is the crystal field scheme under the inclusion of the spin-orbit coupling (SOC). The energy separation between the $J = 1/2$ doublet and the $J = 3/2$ quadruplet is set by the SOC.

spin-orbit-entangled $J = 1/2$ doublet. The candidate materials are often referred as “ $J = 1/2$ Mott insulators”. As the orbital is implicitly involved into the moment, the exchange interaction inherits the orbital character and depends on the bond orientations and the components of the moments. Thus, the exchange interaction is usually not of Heisenberg like. A consequence of this anisotropic interaction is the Kitaev interaction that was popular and led to the development of the field of Kitaev materials. The major advantage of “ $J = 1/2$ Mott insulators” on the model side is to provide extra interactions beyond the simple Heisenberg interaction, and these extra interactions could provide more opportunities to realize interesting quantum phases and orders. While it may be fashionable to name these extra interactions as Kitaev interactions and/or others, we stick to the old convention by Moriya so that the comparison can be a bit more insightful. The exchange interaction for the spin-1/2 operators is always pairwise and quadratic. According to Moriya [3, 84], these interactions are classified as (symmetric) Heisenberg interaction, (antisymmetric) Dzyaloshinskii-Moriya interaction, and (symmetric) pseudo-dipole interaction.

The “ $J = 3/2$ Mott insulator” is realized when one single electron is or three electrons are placed on the lower t_{2g} quadruplet and the system becomes Mott insulating [25, 35–40]. Despite the popularity of the “ $J = 1/2$ Mott insulators”, the “ $J = 3/2$ Mott insulators” did not receive much attention. We do not have any bias towards either of them, and simply address and explain what the nature could provide to us. What are the new features of the “ $J = 3/2$ Mott insulators” from the model side? First of all, $J = 3/2$ local moments provide a larger local Hilbert space than $J = 1/2$ and allow more possibilities for interesting and novel quantum phases and orders. It was conventionally believed that large spin local moments tend to behave more classically. This conventional belief, however, does not really apply to $J = 3/2$ Mott insulators. This comes to our second point below. The conventional Heisenberg model does not generate strong quantum fluctuations as it only changes the spin quantum number by ± 1 , and thus the large spin magnets with a simple Heisenberg model usually behave rather classically. For the $J = 3/2$ Mott insulators, more operators beyond J^x, J^y, J^z are generated in the superexchange processes and interactions due to the inclusion of the orbital degrees of freedom in the $J = 3/2$ local moments via the SOC. These operators are actually generators of the

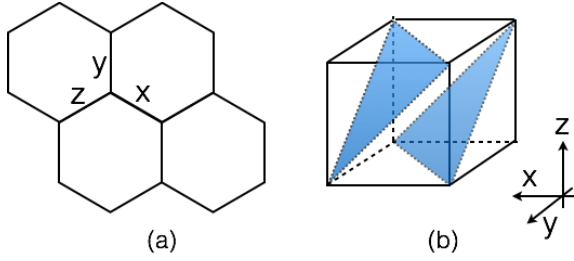


FIG. 4. (a) The honeycomb lattice with “ x, y, z ” bond assignment for the nearest neighbors. (b) The [111] bilayer of the transition metal oxide interfaces.

SU(4) group that are “ 4×4 ” Γ matrices. These Γ matrix operators allow the system to fluctuate more effectively between different spin states and generate stronger quantum fluctuations. This point is similar to the one that has been invoked for high symmetry ultracold atom models in the introduction section (see Sec. I). Thirdly, similar to the “ $J = 1/2$ Mott insulators”, the exchange interaction of the “ $J = 3/2$ Mott insulators” is highly anisotropic and depends on the bond orientation.

Finally, we make a remark that the Γ matrix model for the “ $J = 3/2$ Mott insulators” can be regarded as a parent model for various anisotropic models for the effective spin-1/2 local moments. This is understood by introducing the single-ion anisotropic term and reducing the Γ matrix model into the low-energy manifold favored by the single-ion spin term. This may be made an analogy with the models for the free-electron band structure topology. The Luttinger model [85–92], that uses Γ matrices for $k.p$ theory and gives Luttinger semimetal with a quadratic band touching in 3D, can be regarded as a parent model for generating other models for 3D topological insulators and 3D Weyl semimetal upon introducing strains and magnetism.

In the next section, we will focus on this $J = 3/2$ Mott insulator on the honeycomb structure and explicitly derive the Kugel-Khomskii model.

IV. EMERGENT KUGEL-KHOMSKII PHYSICS IN $J = 3/2$ MOTT INSULATOR

Even though the $J = 3/2$ Mott insulator widely exists in many materials, we here consider a $J = 3/2$ Mott insulator in the honeycomb lattice for the specific demonstration purpose. This is expected to be relevant for the material ZrCl_3 where the Zr^{3+} ions form a honeycomb lattice [40]. It is also relevant for the transition metal oxide bilayer along the [111] lattice direction where each triangular layer is regarded as one sublattice of the honeycomb lattice. As we have explained in the previous section, the requirement for the magnetic ions is to have a $4d^1$ or $5d^1$ electron configuration in an octahedral environment where the SOC is active. To build up a physical model for this honeycomb lattice $J = 3/2$ Mott insulator, we first specify the degree of freedom. Before including the effect of SOC, the local moment is described by a localized

spin-1/2 electron on the three-fold degenerate t_{2g} orbitals at each magnetic ion site. The interaction between the local moments is understood as a standard Kugel-Khomskii superexchange model for the t_{2g} systems. Including the atomic SOC, we express the full model as

$$H = H_{\text{KK}} + H_{\text{SOC}}, \quad (16)$$

where the first term describes the standard Kugel-Khomskii superexchange interaction, and the second term is the on-site atomic SOC. For the z bond in Fig. 4(a), the superexchange interaction has the following form,

$$H_{\text{KK}}^z = \sum_{\langle ij \rangle} J (\mathbf{S}_{i,xy} \cdot \mathbf{S}_{j,xy} + \frac{1}{4} n_{i,xy} n_{j,xy}), \quad (17)$$

where $\mathbf{S}_{i,xy}$ defines the electron spin on the xy orbital with $\mathbf{S}_{i,xy} = \mathbf{S}_i n_{i,xy}$, and $n_{i,xy}$ defines the electron occupation number on the xy orbital. As the xy orbital gives a dominant σ -bonding, the superexchange interaction is primarily given by the exchange process along this σ -bonding. Although some other exchange processes would give extra contributions to the exchange Hamiltonian, we keep the primary contribution for the demonstration purpose. The exchange interactions on other bonds can be written down from a simple permutation. The atomic SOC has the expression,

$$H_{\text{SOC}} = \sum_i -\lambda \mathbf{l}_i \cdot \mathbf{S}_i, \quad (18)$$

where \mathbf{l}_i is the effective orbital angular momentum for the t_{2g} orbital with $l = 1$, and \mathbf{S}_i is the spin-1/2 operator for the localized electron. Interestingly, the Kugel-Khomskii superexchange at this stage is not and actually has little to do with the emergent Kugel-Khomskii physics. To demonstrate how the Kugel-Khomskii physics emerges, we first analyze the energy scales in the system. In Eq. (16), there are only two energy scales, the superexchange coupling and the atomic SOC. In many $4d/5d$ systems, the atomic SOC is often of similar energy scales as the electron bandwidth and the electron correlation. However, in the Mott insulating regime, what is available for a meaningful comparison is the superexchange coupling. This coupling is usually much weaker than the atomic SOC for the $4d/5d$ materials. In the sense of perturbation theory, the atomic SOC is treated as the main Hamiltonian and the superexchange is regarded as the perturbative term. The atomic SOC entangles the orbital angular momentum \mathbf{l} with the spin \mathbf{S} , and leads to a $J = 3/2$ quadruplet on each site. The superexchange interaction is then operating on the degenerate manifold of the $J = 3/2$ local moments. Following the spirit of the degenerate perturbation theory, we project the superexchange model on the degenerate manifold,

$$H_{\text{eff}} = \prod_i \sum_{m_i} |m_i\rangle \langle m_i| \cdot H_{\text{KK}} \cdot \prod_j \sum_{m_j} |m_j\rangle \langle m_j|, \quad (19)$$

where m_i (m_j) is the quantum number of the J_i^z (J_j^z) operator and takes the values of $\pm 1/2, \pm 3/2$. As we explained in the previous section, the effective Hamiltonian can be expressed into a quadratic form in terms of the Γ matrices at each site. The Γ -matrix expression, however, hides the original physical

meaning. In the following, we first express the effective model in the J -basis, and then explain the emergent Kugel-Khomskii physics by expressing it into the form of Kugel-Khomskii interaction. In terms of the J operators, the effective model has the expression,

$$H_{\text{eff}}^z = \sum_{\langle ij \rangle} J (\tilde{S}_{i,xy}^z \cdot \tilde{S}_{j,xy}^z + \frac{1}{4} \tilde{n}_{i,xy} \cdot \tilde{n}_{j,xy}), \quad (20)$$

where we have

$$\tilde{S}_{i,xy}^x = P_{\frac{3}{2}} S_{i,xy}^x P_{\frac{3}{2}} = \frac{J_i^x}{4} - \frac{J_i^z J_i^x J_i^z}{3}, \quad (21)$$

$$\tilde{S}_{i,xy}^y = P_{\frac{3}{2}} S_{i,xy}^y P_{\frac{3}{2}} = \frac{J_i^y}{4} - \frac{J_i^z J_i^y J_i^z}{3}, \quad (22)$$

$$\tilde{S}_{i,xy}^z = P_{\frac{3}{2}} S_{i,xy}^z P_{\frac{3}{2}} = \frac{3J_i^z}{4} - \frac{J_i^x J_i^x J_i^z}{3}, \quad (23)$$

$$\tilde{n}_{i,xy} = P_{\frac{3}{2}} n_{i,xy} P_{\frac{3}{2}} = \frac{3}{4} - \frac{(J_i^z)^2}{3}. \quad (24)$$

Unlike the simple Heisenberg model that only involves the linear spin operators, the effective model involves the spin products with two or three “ J ” operators. These operators are high order magnetic multipolar moments and are able to switch the local spin state from one J state to any other states, and thus quantum fluctuations are strongly enhanced. In terms of the “ J ” operators, the effective model is rather difficult to be tackled with, and the conventional wisdom cannot provide more physical intuition. Instead, we turn to the perspective of the emergent Kugel-Khomskii physics where the previous knowledge and theoretical techniques about the Kugel-Khomskii model can be adapted [3, 4, 10, 93–95]. For this purpose, we merely need to show the Kugel-Khomskii structure and reduce the effective model into the standard Kugel-Khomskii form.

We first make the following mapping between the effective spin states and the fictitious spin and orbital states,

$$|J_i^z = +\frac{3}{2}\rangle \equiv |s_i^z = +\frac{1}{2}, \tau_i^z = +\frac{1}{2}\rangle, \quad (25)$$

$$|J_i^z = +\frac{1}{2}\rangle \equiv |s_i^z = +\frac{1}{2}, \tau_i^z = -\frac{1}{2}\rangle, \quad (26)$$

$$|J_i^z = -\frac{1}{2}\rangle \equiv |s_i^z = -\frac{1}{2}, \tau_i^z = -\frac{1}{2}\rangle, \quad (27)$$

$$|J_i^z = -\frac{3}{2}\rangle \equiv |s_i^z = -\frac{1}{2}, \tau_i^z = +\frac{1}{2}\rangle. \quad (28)$$

To distinguish from the physical spin “ S ”, we use the little “ s ” to label the fictitious spin, and use “ τ ” to label the fictitious orbital. Although τ is labeled as the “orbital”, the transformation under the time reversal differs from the usual orbital degree of freedom. This is because $\mathcal{T}|J_i^z = m\rangle = i^{2m}|J_i^z = -m\rangle$ and \mathcal{T} does not modify the orbital degree of freedom for the usual real orbital wavefunctions. Here, the $|J_i^z = 3/2\rangle$ and $|J_i^z = 1/2\rangle$ have a different sign structure under the time reversal operation. This is the case even if we switch the assignment in Eq. (27) and Eq. (28). With the assignment in the above equa-

tions, the original J related operators can be expressed as

$$\tilde{S}_{i,xy}^x = \frac{1}{3} s_i^x (1 - 2\tau_i^z), \quad (29)$$

$$\tilde{S}_{i,xy}^y = \frac{1}{3} s_i^y (1 - 2\tau_i^z), \quad (30)$$

$$\tilde{S}_{i,xy}^z = \frac{1}{3} s_i^z (1 - 2\tau_i^z), \quad (31)$$

$$\tilde{n}_{i,xy} = \frac{1}{3} (1 - 2\tau_i^z). \quad (32)$$

Collecting all the interactions, we obtain the emergent Kugel-Khomskii model, and the interaction on the other bonds can be generated likewise. This interaction now carries the basic features of the conventional Kugel-Khomskii model with the following expression,

$$H_{\text{eff}}^z = \sum_{\langle ij \rangle} \frac{4J}{9} (s_i \cdot s_j + \frac{1}{4}) (\frac{1}{2} - \tau_i^z) (\frac{1}{2} - \tau_j^z). \quad (33)$$

The couplings on the remaining bonds can be obtained by the symmetry transformation.

V. SU(N) AND SP(N) MAGNETISM OF LARGE SYMMETRIES WITH ULTRACOLD FERMIONS

Ultracold atom physics opens up a whole new opportunity for studying novel quantum phases. Different from electrons, alkali and alkaline-earth atoms often exhibit large hyperfine spins. The $2S + 1$ hyperfine atomic levels certainly form a high representation of the spin SU(2) group. Nevertheless, as we have mentioned in the introduction (see Sec. I), quantum magnetism in cold atomic systems is characterized by strong quantum fluctuations: They are in the large- N regime with N representing the fermion components instead of the large- S regime. A new perspective from the SU(N) and Sp(N) physics is more appropriate to describe the characteristic strong quantum fluctuations, which is closely related to Kugel-Khomskii physics and high energy physics as well [42–47, 50, 51, 96–100].

As for alkaline-earth atoms, their hyperfine-spins completely come from the nuclear spins since their atomic shells are filled. Interactions from atomic scatterings are independent from spin components since the nuclei are deeply inside. This is the microscopic reason of their SU(N) interactions. Nevertheless, for alkali high spin atoms, generally speaking, their interactions are spin-dependent. In this case, the SU(N) symmetry is not generic, and the Sp(N) symmetry is the next highest symmetry [43, 44, 46, 47, 50].

As a concrete example, below we review the simplest case of large-spin quantum magnetism of 4-component fermions, i.e., spin-3/2 fermions. An exact and generic symmetry of Sp(4), or, isomorphically SO(5), was proved in spin-3/2 fermion systems (e.g. ^{132}Cs , ^9Be , ^{135}Ba , ^{137}Ba , ^{201}Hg). Such a high symmetry without fine-tuning is rare, providing a unified view to understand quantum magnetism in different tensor channels, Cooper pairing, and density wave orders [43, 44]. Under fining tuning, the Sp(4) symmetry can be augmented

to SU(4). The generic Sp(4) symmetry plays the role of the SU(2) symmetry in spin-1/2 systems. They are characterized by strong quantum fluctuations brought by Sp(4) and SU(4). We also review the ‘‘baryon-like’’ physics in quantum magnetism. In quantum chromodynamics (QCD), quarks with three components R , G , and B form the fundamental representation of the SU(3) group. Three quarks of all the R , G , B components form a color singlet, a baryon, while, two quarks cannot form a color singlet. Similarly, here the SU(N) fermion systems are characterized by the N -fermion correlations. The consequential multi-fermion clustering instability was studied that N fermions form an SU(N) singlet [97, 101, 102]. Similarly, in an SU(N) quantum magnet, quantum spin fluctuations are dominated by multi-site correlations, whose physics is beyond the two-site one of the SU(2) magnets which are often studied condensed matter systems. It is exciting that in spite of the huge difference of energy scales, the large-spin cold fermions can also exhibit similar physics to that in QCD [96, 98, 103, 104].

A. The spin-3/2 Hubbard model – the generic Sp(4) symmetry

In this part, we review the hidden and generic Sp(4) symmetry of the spin-3/2 fermions. Sp(4) is the double covering group of SO(5), and the relation between them is the same as that between SU(2) and SO(3). For simplicity, we will use Sp(4) and SO(5) interchangeably neglecting their minor difference.

Consider a single-band Hubbard model of spin-3/2 ultra-cold fermions. Its free-fermion part H_0 reads,

$$H_0 = -t \sum_{\langle ij \rangle, \sigma} (\psi_{i\sigma}^\dagger \psi_{j\sigma} + h.c.) - \mu \sum_{i, \sigma} \psi_{i\sigma}^\dagger \psi_{i\sigma}, \quad (34)$$

where ψ_σ is the 4-component fermion spinor operator and σ represents the component indices $s_z = \pm 3/2, \pm 1/2$; $\langle ij \rangle$ denotes the nearest neighboring bonding. The onsite interactions H_{int} are constrained by Pauli’s exclusion principle: The total spin of two spin-3/2 fermions on the same site can only be 0 (singlet) or 2 (quintet), *i.e.*, whose interaction strengths are denoted as U_0 and U_2 , respectively. H_{int} can be expressed in the spin SU(2) language as

$$H_{int} = U_0 \sum_i P_0^\dagger(i) P_0(i) + U_2 \sum_{i, -2 \leq m \leq 2} P_{2m}^\dagger(i) P_{2m}(i), \quad (35)$$

where P_0^\dagger and P_{2m}^\dagger are the pairing operators in the singlet and quintet channels, respectively. Nevertheless, it is more enlightening to formulate it in an explicitly Sp(4) invariant way,

$$H_{int} = \frac{3U_0 + 5U_2}{16} \sum_i [n(i) - 2]^2 + \frac{U_0 - U_2}{4} \sum_{i, 1 \leq a \leq 5} n_a^2(i), \quad (36)$$

where $n = \psi_\alpha^\dagger \psi_\alpha$ is the particle number operator, and n_a is the spin-quadrupole operator defined as

$$n_a = \frac{1}{2} \psi_\alpha^\dagger \Gamma_{\alpha\beta}^a \psi_\beta, \quad (1 \leq a \leq 5). \quad (37)$$

The Γ -matrices are defined as the quadratic forms of the spin-3/2 operators S_x, S_y , and S_z :

$$\Gamma^1 = \frac{1}{\sqrt{3}} (S_x S_y + S_y S_x), \quad (38)$$

$$\Gamma^2 = \frac{1}{\sqrt{3}} (S_z S_x + S_x S_z), \quad (39)$$

$$\Gamma^3 = \frac{1}{\sqrt{3}} (S_z S_y + S_y S_z), \quad (40)$$

$$\Gamma^4 = S_z^2 - \frac{5}{4}, \quad (41)$$

$$\Gamma^5 = \frac{1}{\sqrt{3}} (S_x^2 - S_y^2). \quad (42)$$

They satisfy the anti-commutation relation $\{\Gamma^a, \Gamma^b\} = 2\delta_{ab}$.

It is readily to show that $H_0 + H_{int}$ is Sp(4), or, SO(5) invariant: ψ_α is a 4-component spinor of Sp(4); n is an Sp(4) scalar and the n^a operators form a 5-vector. The latter two are all time-reversal even. The generators of the Sp(4) group are defined as

$$L_{ab} = -\frac{1}{2} \psi_\alpha^\dagger \Gamma_{\alpha\beta}^{ab} \psi_\beta, \quad (43)$$

where Γ^{ab} ’s are defined as the commutators of Γ^a as

$$\Gamma^{ab} = -\frac{i}{2} [\Gamma^a, \Gamma^b] \quad (1 \leq a, b \leq 5). \quad (44)$$

L_{ab} ’s consist of spin and spin-octupole operators [43, 105]. Since they are odd rank spin tensors, they are time-reversal odd. The SO(5) generators L_{ab} , or, the adjoint representation, and its vectors n_a together span the SU(4) algebra. Among them, three diagonal operators commute with each other:

$$L_{15} = \frac{1}{2} (n_{\frac{3}{2}} + n_{\frac{1}{2}} - n_{-\frac{1}{2}} - n_{-\frac{3}{2}}), \quad (45)$$

$$L_{23} = \frac{1}{2} (n_{\frac{3}{2}} - n_{\frac{1}{2}} + n_{-\frac{1}{2}} - n_{-\frac{3}{2}}), \quad (46)$$

$$n_4 = \frac{1}{2} (n_{\frac{3}{2}} - n_{\frac{1}{2}} - n_{-\frac{1}{2}} + n_{-\frac{3}{2}}). \quad (47)$$

In the group theory language, they form a rank-3 Cartan sub-algebra of SU(4). As for the Sp(4) algebra, its Cartan sub-algebra is rank-2 formed only by L_{15} and L_{23} .

B. The superexchanges at quarter-filling

If the repulsive interactions are sufficiently strong, the system enters the Mott-insulating state even at 1/4-filling, *i.e.*, one fermion per site. The low-energy physics lies in the magnetic channel as described by the superexchange model constructed in Ref. 96.

The superexchange energies exist in the bond-spin singlet and quintet channels, denoted as J_0 and J_2 , respectively, whose expressions are obtained via the 2nd order perturbation theory as $J_0 = 4t^2/U_0$ and $J_2 = 4t^2/U_2$. The Heisenberg

model can be expressed in an explicitly SO(5) invariant way as [105]

$$H_{ex} = \sum_{\langle ij \rangle} \left\{ J_L \sum_{1 \leq a < b \leq 5} L_{ab}(i) L_{ab}(j) + J_N \sum_{a=1}^5 n_a(i) n_a(j) \right\}, \quad (48)$$

with $J_L = (J_0 + J_2)/4$ and $J_N = (3J_2 - J_0)/4$. The Sp(4) good quantum numbers are defined as follows:

$$C = \sum_{1 \leq a < b \leq 5} \left\{ \sum_i L_{ab}(i) \right\}^2, \quad (49)$$

$$L_{15}^{tot} = \sum_i L_{15}(i), \quad L_{23}^{tot} = \sum_i L_{23}(i), \quad (50)$$

where C denotes the Sp(4) Casimir of the entire system, and L_{15}^{tot} and L_{23}^{tot} are the corresponding Cartan sub-algebra. C , L_{15}^{tot} and L_{23}^{tot} are the analogues to the total spin square, and the total S_z of an SU(2) system. In fact, Eq. (48) can be formulated in the conventional form as the bi-linear, bi-quadratic and even bi-cubic SU(2) Heisenberg terms:

$$H_{ex} = \sum_{\langle i,j \rangle} c_1 (\vec{S}_i \cdot \vec{S}_j) + c_2 (\vec{S}_i \cdot \vec{S}_j)^2 + c_3 (\vec{S}_i \cdot \vec{S}_j)^3, \quad (51)$$

where $c_{1,2,3}$ can be expressed in terms of $J_{0,2}$. Nevertheless, it is more enlightening to express in the Sp(4) language.

At two different sets of parameter values, Eq. (48) exhibits two different SU(4) symmetries. The first case takes place at $J_0 = J_2$, or, equivalently, $U_0 = U_2$, denoted as SU(4)_A below. Eq. (48) is reduced to the SU(4) Heisenberg model

$$H_A = J \sum_{\langle i,j \rangle} \left\{ L_{ab}(i) L_{ab}(j) + n_a(i) n_a(j) \right\}, \quad (52)$$

for which each site lies in the fundamental representation of SU(4), and $J = J_0/2 = J_2/2$. H_A is equivalent to the SU(4) Kugel-Khomskii type model [6, 103, 106–108] as reviewed in the previous sections.

The second SU(4) symmetry takes place in a bipartite lattice and in the limit of $U_2 \rightarrow +\infty$, i.e., $J_2 = 0$. To see this explicitly, the particle-hole transformation $\psi_\alpha \rightarrow R_{\alpha\beta} \psi_\beta^\dagger$ is performed to one sublattice, and the other sublattice is left unchanged, where R is the charge conjugation matrix

$$R = \begin{pmatrix} 0 & i\sigma_2 \\ i\sigma_2 & 0 \end{pmatrix}. \quad (53)$$

Under this operation, the fundamental representation of SU(4) transforms to its anti-fundamental representation whose Sp(4) generators and vectors become $L'_{ab} = L_{ab}$ and $n'_a = -n_a$. The Sp(4) generators remain invariant under the particle-hole transformation is due to its pseudo-reality. Then Eq. (48) can be recast to

$$H_B = J' \sum_{\langle i,j \rangle} \left\{ L'_{ab}(i) L_{ab}(j) + n'_a(i) n_a(j) \right\}, \quad (54)$$

where $J' = J_0/4$. Eq. (54) is SU(4) invariant again.

The implications of these two SU(4) symmetries are fundamentally different, and both of them have high energy analogues: The physics of SU(4)_A is baryon-like, while that of

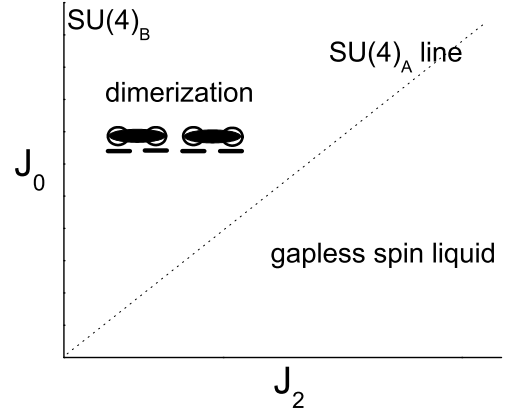


FIG. 5. Phase diagram of a 1D Sp(4) spin chain in terms of J_0 and J_2 with $\tan \theta = J_0/J_2$. The SU(4)_A and SU(4)_B symmetries are located along the lines of $\theta = 45^\circ$ and 90° , respectively. The dimerized spin Peierls phase appears at $90^\circ \geq \theta > 45^\circ$, and the gapless spin liquid phase is located at $45^\circ \geq \theta \geq 0^\circ$. Figure is adapted from Ref. 100.

SU(4)_B is meson-like. In the case of SU(4)_A, every site belongs to the fundamental representation. At least 4 sites are required to form an SU(4) singlet, whose wavefunction is represented as

$$\frac{1}{\sqrt{4!}} \epsilon_{\alpha\beta\gamma\delta} \psi_\alpha^\dagger(1) \psi_\beta^\dagger(2) \psi_\gamma^\dagger(3) \psi_\delta^\dagger(4) |\Omega\rangle, \quad (55)$$

where 1, 2, 3, 4 are site indices, and $\epsilon_{\alpha\beta\gamma\delta}$ is the rank-4 fully antisymmetric tensor, Ω is the particle vacuum. Hence, dramatically different from the SU(2) case, two sites across a bond cannot form a singlet. Hence, quantum magnetism based on H_A exhibits strong features of the 4-site correlation, i.e., a baryon-like state. On the other hand, for the case of SU(4)_B, two sites are able to form an SU(4) singlet via the charge conjugation matrix as

$$\frac{1}{2} R_{\alpha\beta} \psi_\alpha^\dagger(1) \psi_\beta^\dagger(2) |\Omega\rangle. \quad (56)$$

This can be viewed as a large- N version of the usual spin-1/2 SU(2) Heisenberg model.

C. Quantum magnetism of an Sp(4) spin chain

We present the study of quantum magnetism of an Sp(4) spin chain as described by Eq. (48) in 1D. At the level of the spin-3/2 Hubbard model, the phase diagram of 1D Sp(4) symmetric system was already investigated by one of the authors via bosonization [105, 109].

The physics of the Sp(4) magnetism occurs in the strong repulsive interaction regime at the commensurate filling of $1/4$, i.e., one particle per site. The charge gap opens due to the relevance of the $4k_f$ -Umklapp process when the Luttinger parameter $0 < K_c < 1/2$, and then the low energy physics is captured by the Sp(4) superexchange process. It has been shown that the 1D spin-3/2 system exhibits a quantum phase transition at the SU(4) symmetric point of $U_0 = U_2$, or, $J_0 = J_2$:

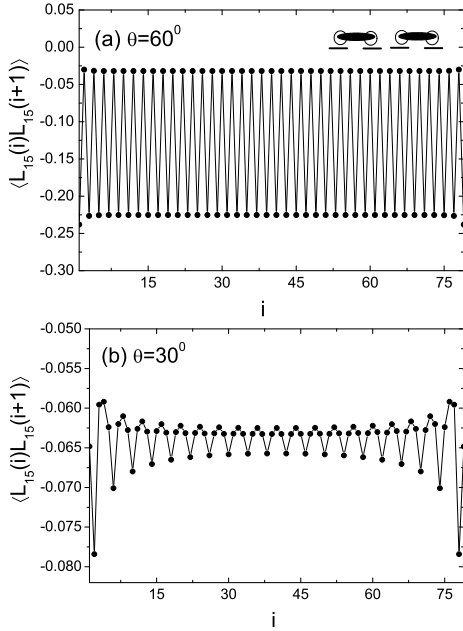


FIG. 6. The DMRG results of the nearest neighbor correlations of $\langle L_{15}(i)L_{15}(i+1) \rangle$ with the open boundary condition. The parameter values are $\theta = 60^\circ$ in (a) and $\theta = 30^\circ$ in (b). A 2-site periodicity appears in (a) and a 4-site periodicity with a power-law decay shows up in (b). Figures are adapted from Ref. 100.

When $U_0 < U_2$ ($J_0 > J_2$), the system develops a spin gap with the presence of the spin Peierls distortion, while at $U_0 \leq U_2$, ($J_0 \leq J_2$), the system enters a gapless spin liquid phase and maintains the translation symmetry [105]. The transition between these two phases is Kosterlitz-Thouless like. The phase diagram is sketched in Fig. 5. For convenience, a parameter angle θ is employed to represent $J_{0,2}$ as

$$J_0 = \sqrt{2} \cos \theta, \quad J_2 = \sqrt{2} \sin \theta. \quad (57)$$

Hence, the gapless spin liquid phase lies at $0 \leq \theta \leq 45^\circ$, while the spin Peierls phase exhibiting dimerization lies at $45^\circ < \theta \leq 90^\circ$.

Below we summarized the results of the Sp(4) spin chain based on the density-matrix-renormalization-group (DMRG) simulations [100]. The ground state spin gap Δ_{sp} is defined as the energy difference between the ground state and the lowest Sp(4) multiplet. The DMRG results show that for the cases of $\theta > 45^\circ$, i.e., $J_2/J_0 < 1$, Δ_{sp} 's saturate to nonzero values in the thermodynamic limit, indicating the opening of spin gaps. On the other hand, Δ_{sp} 's vanish at $\theta \leq 45^\circ$ demonstrating gapless ground states. These results are consistent with the bosonization analysis [109], which shows that the phase boundary is at $\theta = 45^\circ$ with the SU(4)_A symmetry, which is also gapless.

The DMRG results of the nearest neighbor (NN) correlation functions of the Sp(4) generators are presented below. The open boundary condition induces characteristic oscillations. As an example, $\langle L_{15}(i)L_{15}(i+1) \rangle$ is shown in Fig. 6 and correlations of other Sp(4) generators are the same due to the Sp(4) symmetry. For example, at $\theta = 60^\circ$, the dimer pattern is pinned by the open boundary condition. It does not decay

as moving to the center of the chain which implies the presence of long-range-ordering. This is also in agreement with the bosonization analysis [105], and the presence of spin gap in the DMRG simulations. On the other hand, the above correlation exhibits a power-law decay at $\theta = 30^\circ$, showing the gapless ground states. Furthermore, the oscillation periodicity is 4-site. The same oscillation periodicity is the same at $\theta \leq 45^\circ$, which is also in agreement with the dominant $2k_f$ spin correlations in the bosonization analysis.

Next we discuss the two-point correlation functions. A structure factor is defined as

$$S_X(\vec{q}) = \frac{1}{N} \sum_{i,j} e^{i\vec{q} \cdot (\vec{r}_i - \vec{r}_j)} \langle G | X(i)X(j) | G \rangle, \quad (58)$$

where the operator $X = L$, or, n represents an operator in the 10-generator channel, or, the 5-vector channel of the Sp(4) group, respectively. In the gapless spin liquid regime ($0 \leq \theta \leq 45^\circ$), both correlations exhibit the same $2k_f$ 4-site periodicity. They can be expressed in an asymptotic power-law expression as

$$\langle X(i_0)X(i) \rangle \propto \frac{\cos \frac{\pi}{2} |i_0 - i|}{|i_0 - i|^\kappa}. \quad (59)$$

The critical exponents for L and n along the SU(4)_A line ($\theta = 45^\circ$) should be the same, as fitted by $\kappa \approx 1.52$, which is in a good agreement with the value of 1.5 from the bosonization analysis and numerical studies [109–111]. As away from the SU(4)_A line, the degeneracy between L and n is lifted. The simulations show that the critical exponent for the Sp(4) adjoint representation $\kappa_L < 1.5$, while that for the Sp(4) vector channel $\kappa_n > 1.5$.

In the spin gapped dimerization phase with $\theta > 45^\circ$, both correlation functions decay exponentially. Furthermore, the peaks of $S(q)$ with $\theta = 60^\circ$ shift to $q = \pi$, which shows the $4k_f$ charge-density-wave ordering leading to the dimerization.

D. The two-dimensional Sp(4) magnetism – Exact diagonalization on a 4×4 cluster

The physics of the 2D Sp(4) magnetism based on Eq. (48) is very challenging. The global phase remains an unsolved problem. Along the SU(4)_B line, i.e., $\theta = 90^\circ$, quantum Monte Carlo simulations (QMC) show a long-range Néel ordering with a much weaker Néel moment compared to the SU(2) case [112]. However, except this special case, the sign-problem appears and no conclusive results are known. Especially, in the region of $0 < \theta \leq 45^\circ$, the phase is dominated by the baryon-type physics which is quite different from the SU(2) quantum magnetism [96, 107].

Below we review the results for the ground state properties via the exact diagonalization (ED) method. Even though the ED can only be applied to a small 4×4 cluster, the associated ground state profiles at different values of θ still yield valuable information to speculate the thermodynamic limit.

For later convenience, we define the crystal momenta $\Gamma = (0, 0)$, $X = (\pi, 0)$, and $M = (\pi, \pi)$.

1. Low energy spectra

The ED results show that the ground states are always $\text{Sp}(4)$ singlets and are located at the Γ -point. The lowest excitations are located at the X -point when $\theta \leq 63^\circ$, which are also $\text{Sp}(4)$ singlets. This implies the breaking of the translation symmetry of one lattice constant along the x , or, y -direction if this singlet gap vanishes in the thermodynamic limit. This would imply a dimerization pattern and a 4-fold degeneracy of the ground states.

As further increasing θ , this situation qualitatively changes. The low energy excitations consist of states of different $\text{Sp}(4)$ representations, whose energies are nearly degenerate. It is difficult to infer what orders could develop in the thermodynamic limit. At $\theta \geq 72^\circ$, the singlet at X -point is no longer the lowest excitation. The lowest excited states become a set of $\text{Sp}(4)$ 5-vectors located at the Γ -point, whose Casimir $C = 4$. There also exist another set of states located at the M -point, whose energy is very close to the 5-vector's. They form a 10-adjoint representation state with a Casimir $C = 6$. The 5-vector and 10-adjoint states become degenerate at $\text{SU}(4)_B$ point, i.e., $\theta = 90^\circ$. Hence, in the thermodynamic limit, we infer the competition of the long-range ordering of L_{ab} at the wavevector of (π, π) and that of n_a at the wavevector of $(0, 0)$.

Based on the above argument, we would expect a phase transition as follows: A Néel order-like state breaking the $\text{Sp}(4)$ symmetry appears at large values of θ in particular close to 90° ; while an $\text{Sp}(4)$ singlet ground state breaking the translation symmetry exits at momentum X as lowering θ to smaller values.

2. The correlation functions

In this part, we show the further evidence of a Néel-type ground state at large values of θ . Such a region starts from $\theta = 90^\circ$ and extends significantly to $\theta \approx 70^\circ \sim 60^\circ$, although the precise location of the lower boundary is unclear.

This result is based on the structure form factor calculation below. A structure factor converges to a finite value at $L \rightarrow \infty$ in the presence of long-range ordering [112, 113]. For a small cluster, a peak of a structure factor at a characteristic momentum shows the tendency of ordering in the thermodynamic limit.

The structure factor $S_X(\vec{q})$ in the 10-generator channel, i.e., $X = L$, is shown in Fig. 7 (a). When $90^\circ \geq \theta \gtrsim 60^\circ$, $S_L(\vec{q})$ peaks at the M -point implying a tendency of the Néel ordering. In contrast, at $\theta \lesssim 60^\circ$, $S_L(\vec{q})$ distributes relatively smooth over all momenta without dominant peaks. For the 5-vector channel, i.e., $X = n$, the structure factor $S_n(\vec{q})$ is shown in Fig. 7(b). It shows a peak at the Γ -point when $\theta \gtrsim 60^\circ$ roughly in the same range that $S_L(\vec{q})$ develops a peak at the M -point. As θ is lowered, this peak is quickly suppressed, and the distribution of $S_n(\vec{q})$ also becomes smooth in a similar way to that of $S_L(\vec{q})$. Nevertheless, at small values of $\theta < 18^\circ$, it becomes to peak at the M -point, i.e., at the momentum (π, π) .

Now let us check the situation along the two $\text{SU}(4)$ lines. Along $\theta = 90^\circ$, the $\text{SU}(4)_B$ symmetry ensures that relation of

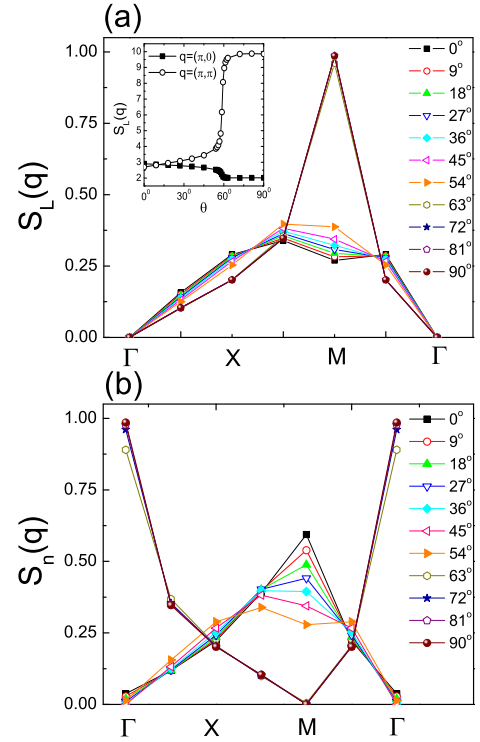


FIG. 7. The structure factors for the 4×4 cluster with (a) $S_L(\vec{q})$ in the $\text{Sp}(4)$ generator sector and (b) $S_n(\vec{q})$ in the $\text{Sp}(4)$ vector sector. The inset in (a) is the comparison between $S_L(\pi, 0)$ and $S_L(\pi, \pi)$ versus θ . Figures are adapted from Ref. 100.

$S_n(\vec{q}) = S_L(\vec{q} + M)$ due to the staggered definition of $\text{Sp}(4)$ vectors n_a in Eq. (54). This relation still approximately holds when θ is close to 90° . The Néel correlation of L_{ab} also extends to a finite regime as θ deviates away from 90° , and in the same regime, n_a exhibits the uniform correlations. Back to the spin language, as $\theta \rightarrow 90^\circ$ the classic energy can be minimized by arranging the two components of $S_z = \pm 3/2$, or, of the other two components of $S_z = \pm 1/2$ in a staggered way. These different configurations are equivalent under the $\text{Sp}(4)$ transformations. In the case of $\text{SU}(4)_A$, i.e., $\theta = 45^\circ$, the 5-vector and the 10-generator channels become degenerate, hence, $S_n(\vec{q}) = S_L(\vec{q})$ for each \vec{q} . As θ deviates away from 45° , S_L and S_n evolve differently.

3. The columnar dimer correlations

In this part, we show the tendency towards a dimerized ground state at intermediate values of θ in the region of $60^\circ < \theta < 70^\circ$. This is consistent with the ED spectra presented before which shows the lowest excitations become $\text{Sp}(4)$ singlets located at the X -point as $\theta \leq 63^\circ$.

To test such a possibility, we define the susceptibilities of translation and rotational symmetry breakings. The following

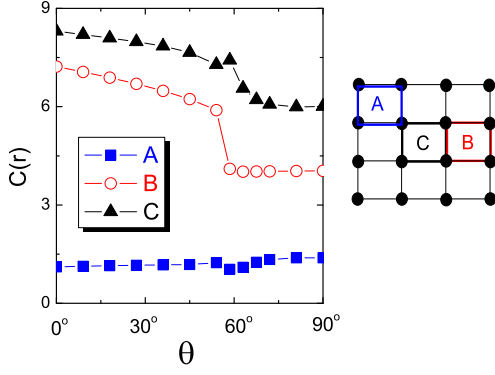


FIG. 8. The local Casimir $C(\vec{r})$ versus θ . The plaquettes A , B and C are depicted in the right.

two perturbations are added to the Hamiltonian Eq. (48), *i.e.*,

$$\hat{O}_{dim}(\vec{Q}) = \sum_i \cos(\vec{Q} \cdot \vec{r}_i) H_{ex}(i, i + \hat{x}), \quad (60)$$

$$\hat{O}_{rot} = \sum_i [H_{ex}(i, i + \hat{x}) - H_{ex}(i, i + \hat{y})]. \quad (61)$$

The former breaks the translation symmetry and the latter breaks the rotation symmetry.

The ED results of susceptibilities associated with \hat{O}_{dim} and \hat{O}_{rot} show that both of them exhibit a peak in the interval of $60^\circ < \theta < 70^\circ$. Although no real divergences exist due to the finite size, sharp peaks in the susceptibilities would imply the tendency of long-range ordering. Hence, the results imply a tendency to breaking both translational and rotational symmetries, which is consistent with a columnar dimerization in this regime in the thermodynamic limit. In contrast, the plaquette ordering does not break the 4-fold rotational symmetry, which is not favored in this regime.

4. The plaquette form factor

We further check the tendency of the plaquette type ordering, *i.e.*, the SU(4) analogy to the baryon state, at small values of θ , *i.e.*, $\theta < 50^\circ \sim 60^\circ$. Previously, the total spin of a plaquette was used to characterize the competing dimer and plaquette orders in the SU(2) quantum antiferromagnets [114]. Here it is generalized to the plaquette Sp(4) Casimir centered at \vec{r} as

$$C(\vec{r}) = \langle G | \sum_{1 \leq a < b \leq 5} \{ \sum_i L_{ab}(i) \}^2 | G \rangle, \quad (62)$$

where i runs over the four sites of this plaquette.

The relation of C versus θ is calculated under the open boundary condition. Based on the symmetry analysis, the values of C for three non-equivalent plaquettes A , B , and C are shown in Fig. 8. $C(A)$ of the corner plaquette is significantly about one order smaller than $C(B)$ and $C(C)$ of the other two plaquettes at small values of θ . This suggests that an Sp(4) plaquette tendency is pinned down by the open boundary. As θ increases above 60° , the contrast decreases which means that the plaquette-type pattern is weakened.

Hence it is likely that there exist a strong plaquette-like correlation at small values of θ in agreement with that proposed by Bossche *et al.* [103, 104] but significantly beyond the SU(4)_A line. It covers the entire region of $\theta < 45^\circ$ and also extends slightly above 45° . Nevertheless, further larger scale calculations are necessary for a conclusion.

E. Quantum plaquette model for the 3D SU(4) magnetism

We have explained that for the SU(4)_A Heisenberg model with each site lying in the fundamental representation, they exhibit the characteristic plaquette correlations. Such a state has been shown as the exact solution to the ground state of a 2-leg ladder model of spin-3/2 fermions [96]. However, due to the geometric constraint, it cannot resonate and is a valence-bond-solid type state.

Here we review the construction of the resonating quantum plaquette model (QPM) model [98, 115], which is analogous to the quantum dimer model for the SU(2) quantum magnet [116, 117]. For the quantum dimer model, there exists a gauge theory description of the Rokhsar-Kivelson (RK) Hamiltonian, which is a compact U(1) gauge theory [117]. QPM also has a similar description as reviewed below, which is a high order gauge field theory. Recently it has received considerable attention in the context of fracton physics [118].

1. The quantum plaquette model

In order to have a resonating QPM, we consider a 3D cubic lattice SU(4) model in the limit that each plaquette has a strong tendency to form a local SU(4) singlet. Then the effective Hilbert space is spanned by all the plaquette configurations. They are subject to the following constraint that every site belongs to one and only one plaquette.

In each unit cube, there exist three flippable configurations: the pairs of plaquettes of left and right, top and bottom, and front and back denoted as A , B and C in Fig. 9, respectively. The Rokhsar-Kivelson (RK) type Hamiltonian is constructed as [116]:

$$H = -t \sum_{\text{each cube}} \{ |A\rangle\langle B| + |B\rangle\langle C| + |B\rangle\langle C| + h.c. \} + V \sum_{\text{each cube}} \{ |A\rangle\langle A| + |B\rangle\langle B| + |C\rangle\langle C| \}, \quad (63)$$

where t is assumed to be positive, and v/t is arbitrary. By defining

$$|Q_{1,2}\rangle = |A\rangle + e^{i\frac{2}{3}\pi}|B\rangle + e^{i\frac{4}{3}\pi}|B\rangle, \quad (64)$$

it is reformulated as

$$H = t \sum_{\text{each cube}} \{ |Q_1\rangle\langle Q_1| + |Q_2\rangle\langle Q_2| \} + (V - 2t) \sum_{\text{each cube}} \{ |A\rangle\langle A| + |B\rangle\langle B| + |C\rangle\langle C| \}. \quad (65)$$

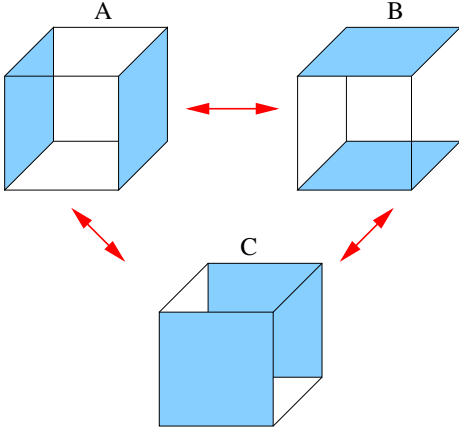


FIG. 9. Three flippable configurations in one cube. Figure is adapted from Ref. 98.

The RK point here corresponds to $v = 2t$. It is easy to show that the ground state here is the equal weight superposition of all the plaquette configurations within the same topological sector that can be connected by local flips. The classical Monte Carlo simulation shows that a crystalline order of resonating cubes at this RK point [115]. At $v/t < 2$, the system favors flippable cubes. For example, as shown in Ref. 115, at $v/t \ll -1$, the ground state exhibit the columnar ordering. At $v > 2t$, both terms in Eq. (65) are positive-definite. Hence, all the configurations without flippable cubes are the ground states. All the transitions between different phases are of the first order.

2. A high order gauge field mapping

It is often useful to extract the low energy physics of strong correlated systems by mapping it to the gauge theory models. In fact, the effective gauge theory of the QPM was constructed as a special one - a high order gauge theory.

Each square face is denoted by the location of its center: $i + \frac{1}{2}\hat{u} + \frac{1}{2}\hat{v}$, where i represents the cubic lattice site and $\hat{u} = \hat{x}, \hat{y}$ and \hat{z} . Each face is associated with a number n and a strong local potential $U(n_{i+\frac{1}{2}\hat{u}+\frac{1}{2}\hat{v}} - \frac{1}{2})^2$ in the limit of $U \rightarrow \infty$, such that the low-energy sector has only either $n = 1$ corresponding to an SU(4) singlet occupation, or $n = 0$, otherwise. The constraint maps to that the summation of n over all the 12 faces connecting to the same site should be 1. We define a rank-2 symmetric traceless tensor electric field

$$E_{i,\mu\nu} = \eta(i)(n_{i+\frac{1}{2}\hat{\mu}+\frac{1}{2}\hat{\nu}} - \frac{1}{2}), \quad (66)$$

where $\eta(i) = \pm 1$ depends on the sublattice that i belongs to, and then the above constraint can be represented as

$$\nabla_x \nabla_y E_{xy} + \nabla_y \nabla_z E_{yz} + \nabla_z \nabla_x E_{zx} = 5\eta(i), \quad (67)$$

where ∇ is the lattice version of the derivative. The canonical conjugate variable of $E_{i,\mu\nu}$ is the vector potential $A_{i,\mu\nu}$, satisfying

$$[E_{i,\mu\nu}, A_{j,\rho\sigma}] = i\delta_{ij}(\delta_{\mu\rho}\delta_{\nu\sigma} + \delta_{\mu\sigma}\delta_{\nu\rho}). \quad (68)$$

$A_{i,\mu\nu}$ can be expressed by the phase variable $\theta_{i+\frac{1}{2}\hat{\mu}+\frac{1}{2}\hat{\nu}}$, which is the canonical conjugate variable to n as $A_{i,\mu\nu} = \eta(i)\theta_{i+\frac{1}{2}\hat{\mu}+\frac{1}{2}\hat{\nu}}$. Because $E_{\mu\nu}$ only takes integer values, $A_{\mu\nu}$ is a compact field with period of 2π .

The plaquette flipping process changes the plaquette occupations. For this purpose, we employ $e^{iA_{j\nu\sigma}}$ which changes the eigenvalue of $E_{i,\mu\nu}$ by 1 since

$$[E_{i,\mu\nu}, e^{iA_{j\nu\sigma}}] = (\delta_{\mu\rho}\delta_{\nu\sigma} + \delta_{\mu\sigma}\delta_{\nu\rho})e^{iA_{j\nu\sigma}}. \quad (69)$$

Then the flipping term is represented as

$$H_t = -t[\cos(\nabla_z A_{xy} - \nabla_x A_{yz}) + \cos(\nabla_x A_{yz} - \nabla_y A_{zx}) + \cos(\nabla_y A_{zx} - \nabla_z A_{xy})]. \quad (70)$$

The associated gauge invariant transformation is $A_{\mu\nu} \rightarrow A_{\mu\nu} + \nabla_\mu \nabla_\nu f$, where f an arbitrary scalar function. The low-energy Hamiltonian of the system can be written as

$$H = H_t + \sum_{\text{each cube}} \{U[E_{xy}^2 + E_{yz}^2 + E_{zx}^2] + V[(\nabla_x E_{yz})^2 + (\nabla_y E_{zx})^2 + (\nabla_z E_{xy})^2]\}, \quad (71)$$

under the constraint of Eq. (67).

The above high order gauge theory is a compact one, and the non-local topological defect excitations is crucial to determine whether its ground state is gapless or gapped. The convenient way for this analysis is by the duality mapping to a height model, such that topological defects are mapped to vertex operators [98]. Due to the proliferation of topological defects, the system is generally gapped for the whole phase diagram of the quantum model, which corresponds to crystalline orders. At the RK point, the ground state correlations map to a 3D classic plaquette model with all allowed configurations equally favorable, then the physics is purely determined by entropy. The crystalline order still develops as an effect of ‘‘order from disorder’’ to take the advantage of the flippable cubes. Nevertheless, it has been shown if an energetic term could add to favor unflippable cube configurations, such that the defect proliferation is suppressed, then a critical phase would be achieved. This is 3D analogue to the celebrated Kosterlitz-Thouless transition.

VI. SUMMARY

In summary, we have reviewed a class of novel Mott insulators in both solid state and ultracold atom systems. In both cases, the local Hilbert states in each unit cell consist of more than two components in contrast to the conventional spin-1/2 Mott insulators. They bear similarities to the orbital-active Mott-insulators but typically do not explicitly exhibit the orbital degree of freedom. These include the breathing/cluster magnets, the effective $J = 3/2$ Mott insulators in various transition metal oxides and rare-earth systems, and the ultracold atom fermion systems with large hyperfine-spins, etc.

The study of this class of novel Mott-insulators will certainly broaden the research scope of quantum magnetism, and

further enrich the activity of exploring novel states of matter. As the consequence of the large local Hilbert space, this class of Mott insulators exhibit the common feature of enhanced quantum fluctuations. Instead of being viewed from the large- S perspective, the appropriate viewpoint should be large- N . The low-energy superexchange models typically go beyond the $SU(2)$ large- S Heisenberg models, and bear similarities to the Kugel-Khomskii models. They are expected to exhibit a variety novel physics including spin-multipolar ordering, "bayone-like" like physics, and even more exotic spin-liquid states.

ACKNOWLEDGMENTS

We are grateful from the previous collaboration and discussion with Leon Balents, Patrick Lee, Fuchun Zhang, Xu-Ping Yao, Rui Luo, Lucile Savary, Rodrigo Pereira, Frédéric Mila, Michael Hermele, Ana Maria Rey, Leo Radzihovsky, Jun Ye, Kaden Hazzard, Salvatore Manmana, Arun Paramekanti, Bruce Gaulin, Yong-Baek Kim, Michel Gingras, George Jackeli, Xiaoqun Wang, Tao Xiang, Yue Yu, Cenke Xu, Jiang-Ping Hu, Shoucheng Zhang, and many others. G.C. is supported by the National Science Foundation of China with Grant No. 92065203, the Ministry of Science and Technology of China with Grants No. 2018YFE0103200, by the Shanghai Municipal Science and Technology Major Project with Grant No. 2019SHZDZX04, and by the Research Grants Council of Hong Kong with General Research Fund Grant No. 17306520. C.W. is supported by the Natural Science Foundation of China through Grant No. 12174317, and No. 11729402.

-
- [1] P. W. Anderson, *Basic notations of condensed matter physics* (The Benjamin/Cummings Publishing Company, Inc., 1984).
- [2] Xie Chen, Zheng-Cheng Gu, Zheng-Xin Liu, and Xiao-Gang Wen, "Symmetry protected topological orders and the group cohomology of their symmetry group," *Physical Review B* **87**, 155114 (2013).
- [3] Sadamichi Maekawa, Takami Tohyama, Stewart E. Barnes, Sumio Ishihara, Wataru Koshibae, and Giniyat Khaliullin, *Physics of Transition Metal Oxides* (Springer-Verlag Berlin Heidelberg, 2004).
- [4] Daniel Khomskii, *Transition Metal Compounds* (Cambridge University Press, 2014).
- [5] "Correlated Systems with Multicomponent Local Hilbert Spaces," KITP Program (2020).
- [6] K. I. Kugel and D. I. Khomskii, *Usp. Fiz. Nauk* **136**, 631 (1982).
- [7] P. W. Anderson, "Antiferromagnetism. Theory of Superexchange Interaction," *Phys. Rev.* **79**, 350–356 (1950).
- [8] Andrzej M. Oleś, "Orbital physics," (2017), [arXiv:1708.07183 \[cond-mat.str-el\]](https://arxiv.org/abs/1708.07183).
- [9] Y. Tokura and N. Nagaosa, "Orbital physics in transition-metal oxides," **288**, 462–468 (2000).
- [10] Giniyat Khaliullin, "Orbital Order and Fluctuations in Mott Insulators," *Progress of Theoretical Physics Supplement* **160**, 155–202 (2005).
- [11] M. Z. Hasan and C. L. Kane, "Colloquium: Topological insulators," *Rev. Mod. Phys.* **82**, 3045–3067 (2010).
- [12] Xiao-Liang Qi and Shou-Cheng Zhang, "Topological insulators and superconductors," *Rev. Mod. Phys.* **83**, 1057–1110 (2011).
- [13] B. Q. Lv, T. Qian, and H. Ding, "Experimental perspective on three-dimensional topological semimetals," *Rev. Mod. Phys.* **93**, 025002 (2021).
- [14] N. P. Armitage, E. J. Mele, and Ashvin Vishwanath, "Weyl and dirac semimetals in three-dimensional solids," *Rev. Mod. Phys.* **90**, 015001 (2018).
- [15] William Witczak-Krempa, Gang Chen, Yong Baek Kim, and Leon Balents, "Correlated quantum phenomena in the strong spin-orbit regime," *Annual Review of Condensed Matter Physics* **5**, 57–82 (2014).
- [16] Luuk J. P. Ament, Michel van Veenendaal, Thomas P. Devereaux, John P. Hill, and Jeroen van den Brink, "Resonant inelastic X-ray scattering studies of elementary excitations," *Rev. Mod. Phys.* **83**, 705–767 (2011).
- [17] J. Schlappa, K. Wohlfeld, K. J. Zhou, M. Mourigal, M. W. Haverkort, V. N. Strocov, L. Hozoi, C. Monney, S. Nishimoto, S. Singh, and et al., "Spin-orbital separation in the quasi-one-dimensional Mott insulator Sr_2CuO_3 ," *Nature* **485**, 82–85 (2012).
- [18] Gang Chen, Hae-Young Kee, and Yong Baek Kim, "Cluster Mott insulators and two Curie-Weiss regimes on an anisotropic kagome lattice," *Phys. Rev. B* **93**, 245134 (2016).
- [19] Gang Chen and Patrick A. Lee, "Emergent orbitals in the cluster Mott insulator on a breathing kagome lattice," *Phys. Rev. B* **97**, 035124 (2018).
- [20] K. Kimura, S. Nakatsuji, and T. Kimura, "Experimental realization of a quantum breathing pyrochlore antiferromagnet," *Phys. Rev. B* **90**, 060414 (2014).
- [21] J. G. Rau, L. S. Wu, A. F. May, L. Poudel, B. Winn, V. O. Garlea, A. Huq, P. Whitfield, A. E. Taylor, M. D. Lumsden, M. J. P. Gingras, and A. D. Christianson, "Anisotropic Exchange within Decoupled Tetrahedra in the Quantum Breathing Pyrochlore $Ba_3Yb_2Zn_5O_{11}$," *Phys. Rev. Lett.* **116**, 257204 (2016).
- [22] Lucile Savary, Xiaoqun Wang, Hae-Young Kee, Yong Baek Kim, Yue Yu, and Gang Chen, "Quantum spin ice on the breathing pyrochlore lattice," *Phys. Rev. B* **94**, 075146 (2016).
- [23] S. A. Nikolaev, I. V. Solov'yev, and S. V. Streltsov, "Quantum spin liquid and cluster Mott insulator phases in the Mo_3O_8 magnets," *npj Quantum Mater.* **6**, 25 (2021).
- [24] J. P. Sheckelton, J. R. Neilson, D. G. Soltan, and T. M. McQueen, "Possible valence-bond condensation in the frustrated cluster magnet $LiZn_2Mo_3O_8$," *Nature Materials* **11**, 4937496 (2012).
- [25] Heung-Sik Kim, Jino Im, Myung Joon Han, and Hosub Jin, "Spin-orbital entangled molecular J_{eff} states in lacunar spinel compounds," *Nature Communications* **5**, 3988 (2014).
- [26] Xu-Ping Yao, Xiao-Tian Zhang, Yong Baek Kim, Xiaoqun Wang, and Gang Chen, "Clusterization transition between cluster mott insulators on a breathing kagome lattice," *Phys.*

- [Rev. Research 2, 043424 \(2020\).](#)
- [27] M. Mourigal, W. T. Fuhrman, J. P. Sheckelton, A. Wartelle, J. A. Rodriguez-Rivera, D. L. Abernathy, T. M. McQueen, and C. L. Broholm, “Molecular Quantum Magnetism in $\text{LiZn}_2\text{Mo}_3\text{O}_8$,” *Phys. Rev. Lett.* **112**, 027202 (2014).
- [28] Sachith Dissanayake, Zhenzhong Shi, Jeffrey G. Rau, Rabinranath Bag, William Steinhart, Nicholas P. Butch, Matthias Frontzek, Andrey Podlesnyak, David Graf, Casey Marjerrison, Jue Liu, Michel J. P. Gingras, and Sara Haravifard, “Towards understanding the magnetic properties of the breathing pyrochlore compound $\text{Ba}_3\text{Yb}_2\text{Zn}_5\text{O}_{11}$: A single crystal study,” (2021), [arXiv:2111.06293 \[cond-mat.str-el\]](#).
- [29] Hamid R. Molavian, Michel J. P. Gingras, and Benjamin Canals, “Dynamically Induced Frustration as a Route to a Quantum Spin Ice State in $\text{Tb}_2\text{Ti}_2\text{O}_7$ via Virtual Crystal Field Excitations and Quantum Many-Body Effects,” *Phys. Rev. Lett.* **98**, 157204 (2007).
- [30] M. J. P. Gingras, B. C. den Hertog, M. Faucher, J. S. Gardner, S. R. Dunsiger, L. J. Chang, B. D. Gaulin, N. P. Raju, and J. E. Greedan, “Thermodynamic and single-ion properties of Tb^{3+} within the collective paramagnetic-spin liquid state of the frustrated pyrochlore antiferromagnet $\text{Tb}_2\text{Ti}_2\text{O}_7$,” *Phys. Rev. B* **62**, 6496–6511 (2000).
- [31] B. D. Gaulin, J. S. Gardner, P. A. McClarty, and M. J. P. Gingras, “Lack of evidence for a singlet crystal-field ground state in the magnetic pyrochlore $\text{Tb}_2\text{Ti}_2\text{O}_7$,” *Phys. Rev. B* **84**, 140402 (2011).
- [32] K. Fritsch, K. A. Ross, Y. Qiu, J. R. D. Copley, T. Guidi, R. I. Bewley, H. A. Dabkowska, and B. D. Gaulin, “Antiferromagnetic spin ice correlations at $(\frac{1}{2}, \frac{1}{2}, \frac{1}{2})$ in the ground state of the pyrochlore magnet $\text{Tb}_2\text{Ti}_2\text{O}_7$,” *Phys. Rev. B* **87**, 094410 (2013).
- [33] K. Fritsch, E. Kermarrec, K. A. Ross, Y. Qiu, J. R. D. Copley, D. Pomaranski, J. B. Kycia, H. A. Dabkowska, and B. D. Gaulin, “Temperature and magnetic field dependence of spin-ice correlations in the pyrochlore magnet $\text{Tb}_2\text{Ti}_2\text{O}_7$,” *Phys. Rev. B* **90**, 014429 (2014).
- [34] Changle Liu, Fei-Ye Li, and Gang Chen, “Upper branch magnetism in quantum magnets: Collapses of excited levels and emergent selection rules,” *Phys. Rev. B* **99**, 224407 (2019).
- [35] Gang Chen, Rodrigo Pereira, and Leon Balents, “Exotic phases induced by strong spin-orbit coupling in ordered double perovskites,” *Phys. Rev. B* **82**, 174440 (2010).
- [36] A. Paramekanti, D. D. Maharaj, and B. D. Gaulin, “Octupolar order in d -orbital Mott insulators,” *Phys. Rev. B* **101**, 054439 (2020).
- [37] Judit Romhányi, Leon Balents, and George Jackeli, “Spin-Orbit Dimers and Noncollinear Phases in d^1 Cubic Double Perovskites,” *Phys. Rev. Lett.* **118**, 217202 (2017).
- [38] Yakui Weng and Shuai Dong, “Manipulation of $J_{\text{eff}} = \frac{3}{2}$ states by tuning the tetragonal distortion,” *Phys. Rev. B* **104**, 165150 (2021).
- [39] Yakui Weng, Xing’ao Li, and Shuai Dong, “Strong tuning of magnetism and electronic structure by spin orientation,” *Phys. Rev. B* **102**, 180401 (2020).
- [40] Masahiko G. Yamada, Masaki Oshikawa, and George Jackeli, “Emergent $\text{SU}(4)$ Symmetry in $\alpha\text{-ZrCl}_3$ and Crystalline Spin-Orbital Liquids,” *Phys. Rev. Lett.* **121**, 097201 (2018).
- [41] Andrzej M. Oles, “Spin-orbital physics in transition metal oxides,” (2009), [arXiv:0904.1297 \[cond-mat.str-el\]](#).
- [42] A. V. Gorshkov, M. Hermele, V. Gurarie, C. Xu, P. S. Julianne, J. Ye, P. Zoller, E. Demler, M. D. Lukin, and A. M. Rey, “Two-orbital $\text{SU}(N)$ magnetism with ultracold alkaline-earth atoms,” *Nature Physics* **6**, 289 (2010).
- [43] Congjun Wu, Jiangping Hu, and Shoucheng Zhang, “Exact $\text{SO}(5)$ symmetry in the spin-3/2 fermionic system,” *Phys. Rev. Lett.* **91**, 186402 (2003).
- [44] Congjun Wu, “Hidden symmetry and quantum phases in spin-3/2 cold atomic systems,” *Modern Physics Letters B* **20**, 1707–1738 (2006).
- [45] D. Controzzi and A. M. Tsvelik, “Exactly Solvable Model for Isospin $S = 3/2$ Fermionic Atoms on an Optical Lattice,” *Phys. Rev. Lett.* **96**, 097205 (2006).
- [46] Congjun Wu, “Exotic many-body physics with large-spin fermi gases,” *Physics* **3**, 92 (2010).
- [47] Congjun Wu, “Mott made easy,” *Nat. Phys., New and Views* **8**, 784 (2012).
- [48] B. J. DeSalvo, M. Yan, P. G. Mickelson, Y. N. Martinez de Escobar, and T. C. Killian, “Degenerate Fermi Gas of ^{87}Sr ,” *Phys. Rev. Lett.* **105**, 030402 (2010).
- [49] Shintaro Taie, Rekishu Yamazaki, Seiji Sugawa, and Yoshiro Takahashi, “An $\text{SU}(6)$ Mott insulator of an atomic Fermi gas realized by large-spin Pomeranchuk cooling,” *Nature Physics* **8**, 825–830 (2012).
- [50] M. A. Cazalilla, A. F. Ho, and M. Ueda, “Ultracold gases of ytterbium: ferromagnetism and Mott states in an $\text{SU}(6)$ Fermi system,” *New J. Phys.* **11**, 103033 (2009).
- [51] Michael Hermele, Victor Gurarie, and Ana Maria Rey, “Mott Insulators of Ultracold Fermionic Alkaline Earth Atoms: Underconstrained Magnetism and Chiral Spin Liquid,” *Phys. Rev. Lett.* **103**, 135301 (2009).
- [52] J. B. Goodenough, *Magnetism and Chemical Bond* (Interscience, New York/London, 1963).
- [53] J. Kanamori, “Theory of the Magnetic Properties of Ferrous and Cobaltous Oxides, I,” *Progress of Theoretical Physics* **17**, 177–196 (1957).
- [54] A. Joshi, M. Ma, F. Mila, D. N. Shi, and F. C. Zhang, “Elementary excitations in magnetically ordered systems with orbital degeneracy,” *Phys. Rev. B* **60**, 6584–6587 (1999).
- [55] John B. Goodenough, “Spin-Orbit-Coupling Effects in Transition-Metal Compounds,” *Phys. Rev.* **171**, 466–479 (1968).
- [56] Gang Chen and Leon Balents, “Spin-orbit effects in $\text{Na}_4\text{Ir}_3\text{O}_8$: A hyper-kagome lattice antiferromagnet,” *Phys. Rev. B* **78**, 094403 (2008).
- [57] Amalia I. Coldea and Matthew D. Watson, “The Key Ingredients of the Electronic Structure of FeSe ,” *Annual Review of Condensed Matter Physics* **9**, 125–146 (2018).
- [58] Andrey Chubukov, “Pairing Mechanism in Fe-Based Superconductors,” *Annual Review of Condensed Matter Physics* **3**, 57–92 (2012).
- [59] Paul C. Canfield and Sergey L. Bud’ko, “FeAs-Based Superconductivity: A Case Study of the Effects of Transition Metal Doping on BaFe_2As_2 ,” *Annual Review of Condensed Matter Physics* **1**, 27–50 (2010).
- [60] Anna E Bohmer and Andreas Kreisel, “Nematicity, magnetism and superconductivity in FeSe ,” *Journal of Physics: Condensed Matter* **30**, 023001 (2017).
- [61] Andreas Kreisel, Peter Hirschfeld, and Brian Andersen, “On the Remarkable Superconductivity of FeSe and Its Close Cousins,” *Symmetry* **12**, 1402 (2020).
- [62] Fa Wang, Steven A. Kivelson, and Dung-Hai Lee, “Nematicity and quantum paramagnetism in FeSe ,” *Nature Physics* **11**, 959–963 (2015).
- [63] Hsiang-Hsuan Hung, Can-Li Song, Xi Chen, Xucun Ma, Qikun Xue, and Congjun Wu, “Anisotropic vortex lattice structures in the FeSe superconductor,” *Phys. Rev. B* **85**, 104510 (2012).

- [64] Defa Liu, Cong Li, Jianwei Huang, Bin Lei, Le Wang, Xianxin Wu, Bing Shen, Qiang Gao, Yuxiao Zhang, Xu Liu, Yong Hu, Yu Xu, Aiji Liang, Jing Liu, Ping Ai, Lin Zhao, Shaolong He, Li Yu, Guodong Liu, Yiyuan Mao, Xiaoli Dong, Xiaowen Jia, Fengfeng Zhang, Shenjin Zhang, Feng Yang, Zhimin Wang, Qinqun Peng, Youguo Shi, Jiangping Hu, Tao Xiang, Xianhui Chen, Zuyan Xu, Chuangtian Chen, and X. J. Zhou, “Orbital Origin of Extremely Anisotropic Superconducting Gap in Nematic Phase of FeSe Superconductor,” *Phys. Rev. X* **8**, 031033 (2018).
- [65] CL Song, YL Wang, P Cheng, YP Jiang, W Li, Zhang T, Z Li, K He, L Wang, JF Jia, HH Hung, C Wu, X Ma, X Chen, and Xue QK, “Direct observation of nodes and twofold symmetry in FeSe superconductor,” *Science* **332**, 1410 (2011).
- [66] Joel S. Miller and Dante Gatteschi, “Molecule-based magnets,” *Chem. Soc. Rev.* **40**, 3065–3066 (2011).
- [67] Dante Gatteschi and Roberta Sessoli, “Molecular based magnetic materials,” *Journal of Magnetism and Magnetic Materials* **104-107**, 2092–2095 (1992).
- [68] Maniaki, Diamantoula and Pilichos, Evangelos and Perlepes, Spyros P., “Coordination Clusters of 3d-Metals That Behave as Single-Molecule Magnets (SMMs): Synthetic Routes and Strategies,” *Frontiers in Chemistry* **6**, 461 (2018).
- [69] Y. Shimizu, K. Miyagawa, K. Kanoda, M. Maesato, and G. Saito, “Spin Liquid State in an Organic Mott Insulator with a Triangular Lattice,” *Phys. Rev. Lett.* **91**, 107001 (2003).
- [70] Kazuma Nakamura, Yoshihide Yoshimoto, Taichi Kosugi, Ryotaro Arita, and Masatoshi Imada, “Ab initio Derivation of Low-Energy Model for κ -ET Type Organic Conductors,” *Journal of the Physical Society of Japan* **78**, 083710 (2009).
- [71] Yoshihiko Okamoto, Goran J. Nilsen, Taishi Nakazono, and Zenji Hiroi, “Magnetic Phase Diagram of the Breathing Pyrochlore Antiferromagnet $\text{LiGa}_{1-x}\text{In}_x\text{Cr}_4\text{O}_8$,” *Journal of the Physical Society of Japan* **84**, 043707 (2015).
- [72] F. Mila, “Low-Energy Sector of the $S = 1/2$ Kagome Antiferromagnet,” *Phys. Rev. Lett.* **81**, 2356–2359 (1998).
- [73] J. Zhang, K. Fritsch, Z. Hao, B. V. Bagheri, M. J. P. Gingras, G. E. Granroth, P. Jiramongkolchai, R. J. Cava, and B. D. Gaulin, “Neutron spectroscopic study of crystal field excitations in $\text{Tb}_2\text{Ti}_2\text{O}_7$ and $\text{Tb}_2\text{Sn}_2\text{O}_7$,” *Phys. Rev. B* **89**, 134410 (2014).
- [74] Sylvain Petit, Pierre Bonville, Isabelle Mirebeau, Hannu Mutka, and Julien Robert, “Spin dynamics in the ordered spin ice $\text{Tb}_2\text{Sn}_2\text{O}_7$,” *Phys. Rev. B* **85**, 054428 (2012).
- [75] I. Mirebeau, P. Bonville, and M. Hennion, “Magnetic excitations in $\text{Tb}_2\text{Sn}_2\text{O}_7$ and $\text{Tb}_2\text{Ti}_2\text{O}_7$ as measured by inelastic neutron scattering,” *Phys. Rev. B* **76**, 184436 (2007).
- [76] Jiří Chaloupka, George Jackeli, and Giniyat Khaliullin, “Kitaev-Heisenberg Model on a Honeycomb Lattice: Possible Exotic Phases in Iridium Oxides A_2IrO_3 ,” *Phys. Rev. Lett.* **105**, 027204 (2010).
- [77] G. Jackeli and G. Khaliullin, “Mott Insulators in the Strong Spin-Orbit Coupling Limit: From Heisenberg to a Quantum Compass and Kitaev Models,” *Phys. Rev. Lett.* **102**, 017205 (2009).
- [78] K. W. Plumb, J. P. Clancy, L. J. Sandilands, V. Vijay Shankar, Y. F. Hu, K. S. Burch, Hae-Young Kee, and Young-June Kim, “ α - RuCl_3 : A spin-orbit assisted Mott insulator on a honeycomb lattice,” *Phys. Rev. B* **90**, 041112 (2014).
- [79] Huimei Liu, Jiří Chaloupka, and Giniyat Khaliullin, “Kitaev Spin Liquid in 3d Transition Metal Compounds,” *Phys. Rev. Lett.* **125**, 047201 (2020).
- [80] Huimei Liu and Giniyat Khaliullin, “Pseudospin exchange interactions in d^7 cobalt compounds: Possible realization of the Kitaev model,” *Phys. Rev. B* **97**, 014407 (2018).
- [81] Yukitoshi Motome, Ryoya Sano, Seonghoon Jang, Yusuke Sugita, and Yasuyuki Kato, “Materials design of Kitaev spin liquids beyond the Jackeli-Khaliullin mechanism,” *Journal of Physics: Condensed Matter* **32**, 404001 (2020).
- [82] Ryoya Sano, Yasuyuki Kato, and Yukitoshi Motome, “Kitaev-Heisenberg Hamiltonian for high-spin d^7 Mott insulators,” *Phys. Rev. B* **97**, 014408 (2018).
- [83] M. Elliot, P. A. McClarty, D. Prabhakaran, R. D. Johnson, H. C. Walker, P. Manuel, and R. Coldea, “Order-by-disorder from bond-dependent exchange and intensity signature of nodal quasiparticles in a honeycomb cobaltate,” *Nature Communications* **12** (2021), 10.1038/s41467-021-23851-0.
- [84] Tôru Moriya, “Anisotropic superexchange interaction and weak ferromagnetism,” *Phys. Rev.* **120**, 91–98 (1960).
- [85] J. M. Luttinger and W. Kohn, “Motion of Electrons and Holes in Perturbed Periodic Fields,” *Phys. Rev.* **97**, 869–883 (1955).
- [86] András L. Szabó, Roderich Moessner, and Bitan Roy, “Interacting spin- $\frac{3}{2}$ fermions in a Luttinger semimetal: Competing phases and their selection in the global phase diagram,” *Phys. Rev. B* **103**, 165139 (2021).
- [87] Xu-Ping Yao and Gang Chen, “ $\text{Pr}_2\text{Ir}_2\text{O}_7$: When Luttinger Semimetal Meets Melko-Hertog-Gingras Spin Ice State,” *Phys. Rev. X* **8**, 041039 (2018).
- [88] GiBaik Sim, Archana Mishra, Moon Jip Park, Yong Baek Kim, Gil Young Cho, and SungBin Lee, “Multipolar superconductivity in Luttinger semimetals,” *Phys. Rev. Research* **2**, 023416 (2020).
- [89] Eun-Gook Moon, Cenke Xu, Yong Baek Kim, and Leon Balents, “Non-Fermi-Liquid and Topological States with Strong Spin-Orbit Coupling,” *Phys. Rev. Lett.* **111**, 206401 (2013).
- [90] Maxim Kharitonov, Julian-Benedikt Mayer, and Ewelina M. Hankiewicz, “Universality and Stability of the Edge States of Chiral-Symmetric Topological Semimetals and Surface States of the Luttinger Semimetal,” *Phys. Rev. Lett.* **119**, 266402 (2017).
- [91] Bitan Roy, Sayed Ali Akbar Ghorashi, Matthew S. Foster, and Andriy H. Nevidomskyy, “Topological superconductivity of spin-3/2 carriers in a three-dimensional doped Luttinger semimetal,” *Phys. Rev. B* **99**, 054505 (2019).
- [92] Igor Boettcher and Igor F. Herbut, “Unconventional Superconductivity in Luttinger Semimetals: Theory of Complex Tensor Order and the Emergence of the Uniaxial Nematic State,” *Phys. Rev. Lett.* **120**, 057002 (2018).
- [93] A. B. Harris, Taner Yildirim, Amnon Aharony, Ora Entin-Wohlman, and I. Ya. Korenblit, “Unusual Symmetries in the Kugel-Khomskii Hamiltonian,” *Phys. Rev. Lett.* **91**, 087206 (2003).
- [94] G. Khaliullin and V. Oudovenko, “Spin and orbital excitation spectrum in the Kugel-Khomskii model,” *Phys. Rev. B* **56**, R14243–R14246 (1997).
- [95] S. Di Matteo, G. Jackeli, C. Lacroix, and N. B. Perkins, “Valence-bond crystal in a pyrochlore antiferromagnet with orbital degeneracy,” *Phys. Rev. Lett.* **93**, 077208 (2004).
- [96] S. Chen, C. Wu, Y. P. Wang, and S. C. Zhang, “Exact spontaneous plaquette ground states for high-spin ladder models,” *Phys. Rev. B* **72**, 214428 (2005).
- [97] Congjun Wu and Shoucheng Zhang, “A sufficient condition for the absence of the sign problem in the fermionic quantum Monte-Carlo algorithm,” *Phys. Rev. B* **71**, 155115 (2005).
- [98] Cenke Xu and Congjun Wu, “Resonating plaquette phases in $\text{SU}(4)$ Heisenberg antiferromagnet,” *Phys. Rev. B* **77**, 134449 (2008).

- [99] Xu-Ping Yao, Yonghao Gao, and Gang Chen, “Topological chiral spin liquids and competing states in triangular lattice $SU(N)$ Mott insulators,” *Phys. Rev. Research* **3**, 023138 (2021).
- [100] Hsiang-Hsuan Hung, Yupeng Wang, and Congjun Wu, “Quantum magnetism in ultracold alkali and alkaline-earth fermion systems with symplectic symmetry,” *Phys. Rev. B* **84**, 054406 (2011).
- [101] A. Rapp, G. Zarand, C. Honerkamp, and W. Hofstetter, “Color superfluidity and “baryon” formation in ultracold fermions,” *Phys. Rev. Lett.* **98**, 160405 (2007).
- [102] P. Lecheminant, P. Azaria, and E. Boulat, “Competing orders in one-dimensional half-integer fermionic cold atoms: A conformal field theory approach,” *Nucl. Phys. B* **798**, 443 (2008).
- [103] M. V. D. Bossche, F. C. Zhang, and F. Mila, “Plaquette Ground State in the Two-dimensional $SU(4)$ Spin-Orbital Model,” *Eur. Phys. J. B* **17**, 367 (2000).
- [104] A. Mishra, M. Ma, and F. C. Zhang, “Plaquette ordering in $SU(4)$ antiferromagnets,” *Phys. Rev. B* **65**, 214411 (2002).
- [105] Congjun Wu, “Hidden symmetry and quantum phases in spin-3/2 cold atomic systems,” *Mod. Phys. Lett. B* **20**, 1707 (2006).
- [106] B. Sutherland, “Model for a multicomponent quantum system,” *Phys. Rev. B* **12**, 3795–3805 (1975).
- [107] Y. Q. Li, Michael Ma, D. N. Shi, and F. C. Zhang, “ $SU(4)$ Theory for Spin Systems with Orbital Degeneracy,” *Phys. Rev. Lett.* **81**, 3527 (1998).
- [108] Mathias van den Bossche, P. Azaria, P. Lecheminant, and F. Mila, “Spontaneous Plaquette Formation in the $SU(4)$ Spin-Orbital Ladder,” *Phys. Rev. Lett.* **86**, 4124 (2001).
- [109] Congjun Wu, “Competing orders in one dimensional spin 3/2 fermionic systems,” *Phys. Rev. Lett.* **95**, 266404 (2005).
- [110] Y. Yamashita, N. Shibata, and K. Ueda, “ $SU(4)$ spin-orbit critical state in one dimension,” *Phys. Rev. B* **58**, 9114 (1998).
- [111] P. Azaria, A. O. Gogolin, P. Lecheminant, and A. A. Nersisyan, “One-Dimensional $SU(4)$ Spin-Orbital Model: A Low-Energy Effective Theory,” *Phys. Rev. Lett.* **83**, 624 (1999).
- [112] K. Harada, N. Kawashima, and M. Troyer, “Néel and Spin-Peierls Ground States of Two-Dimensional $SU(N)$ Quantum Antiferromagnets,” *Phys. Rev. Lett.* **90**, 117203 (2003).
- [113] H. J. Schulz and T. A. L. Ziman, “Finite-size scaling for the two-dimensional frustrated quantum heisenberg antiferromagnet,” *Europhys. Lett.* **18**, 355 (1992).
- [114] J. Richter and N. B. Ivanov, “Zero-temperature quantum disorder in spin systems by competition between dimer and plaquette bonds,” *Czechoslovak J. Phys.* **46**, 1919 (1996).
- [115] S. Pankov, R. Moessner, and S. L. Sondhi, “Resonating singlet valence plaquettes,” *Phys. Rev. B* **76**, 104436 (2007).
- [116] Daniel S. Rokhsar and Steven A. Kivelson, “Superconductivity and the quantum hard-core dimer gas,” *Phys. Rev. Lett.* **61**, 2376–2379 (1988).
- [117] Eduardo H. Fradkin and Steven Kivelson, “Short Range Resonating Valence Bond Theories and Superconductivity,” *Mod. Phys. Lett. B* **4**, 225 (1990).
- [118] Rahul M. Nandkishore and Michael Hermele, “Fractons,” *Annual Review of Condensed Matter Physics* **10**, 295–313 (2019).